

A Combined Experimental-Numerical Rheometric and Mechanical Characterization of EPM/EPDM Rubber for Medium Voltage Cable Applications Vulcanized with Peroxides

Gabriele Milani,¹ Andrea Galanti,² Camillo Cardelli,³ Federico Milani⁴

¹Politecnico di Milano, Piazza Leonardo da Vinci 32, 20133 Milan, Italy

²Mixer Compounds Spa, Via Chiara 6/C 48012 Villa Prati di Bagnacavallo (RA), Italy

³IPOOL Srl, Ripa Castel Traetti, Pisa, Italy

⁴Chem.Co consultant, Via J.F. Kennedy 2, 45030 Occhiobello (RO), Italy

Correspondence to: G. Milani (E-mail: gabriele.milani@polimi.it)

ABSTRACT: The vulcanization of medium and high voltage (M-H V) cables is an important industrial application where manufacturers use principally EPM/EPDM, crosslinked polyethylene (XLPE) and now also thermoplastic rubbers. In the present article, an EPDM compound for medium voltage cables—normally distributed to producers in pellets and ready to be cured—is considered and several experimental tests (rheometer curves and mechanical characterizations) are conducted changing controlled curing temperature, peroxide type and peroxide concentration. In particular, tests are replicated in a temperature range between 160 and 200°C, with data provided every 20°C, using two different peroxides, a mixture of three commercial peroxides at five different concentrations. A huge amount of experimental data (cure curves) is obtained (one for each temperature, peroxide used and concentration) and results are critically compared one each other, to have a quantitative insight into the most effective temperature and peroxide to be used during this kind of vulcanization, with the aim of maximizing vulcanization velocity, final torque reached and mechanical properties of cured rubber. The comprehensive experimental study proposed is finally assessed from a numerical point of view, utilizing a complex kinetic scheme constituted by reactions occurring in series and parallel, which allows estimating numerically the vulcanization degree by means of a single second order nonlinear differential equation, with unknown parameters determined through non-linear least squares fitting, with target data represented by experimental rheometer curves. The experimental fitting is almost perfect for all the cases analyzed and is aimed at predicting (without an expensive experimentation) the most suitable production parameters (e.g., curing time and temperature) to guarantee improved mechanical properties and a good aging resistance of the items. In addition, the numerical approach could allow finding the most suitable recipe, also in presence of mixtures of peroxides, able to provide items with a uniform vulcanization level. © 2013 Wiley Periodicals, Inc. *J. Appl. Polym. Sci.* **2014**, *131*, 40075.

KEYWORDS: crosslinking; kinetics; mechanical properties; rubber; theory and modeling

Received 29 August 2013; accepted 15 October 2013

DOI: 10.1002/app.40075

INTRODUCTION

The industrial production of medium and high voltage electric cables exhibits some well-known critical processing steps, needing a comprehensive and combined numerical and experimental insight to be well understood.

One of the most diffused materials utilized for electric cables insulation is EPDM with low unsaturation level and suitable dielectric properties, good ageing resistance, and good mechanical strength.¹ To maximize as well as homogenize as close as possible the crosslinking degree of these items, peroxides are preferred to sulfur, the former curing agents guaranteeing in

general much higher performance and a more stable—from a thermodynamic standpoint—link between parallel chains. It is well known, indeed, that the carbon-carbon bond resulting from peroxide crosslinking is more stable (bond energy equal to 83.1 kcal mole⁻¹) than both the carbon-sulfur bond (62 kcal mole⁻¹) and the sulfur-sulfur bond (50.9 kcal mole⁻¹) formed during sulfur vulcanization.²

For this reason, it can be stated that the curing process of medium and high voltage electric cables with EPM/EPDM rubber having low molecular weight (Mooney viscosity ML), ethylene high content and low-medium amount of ter-monomer

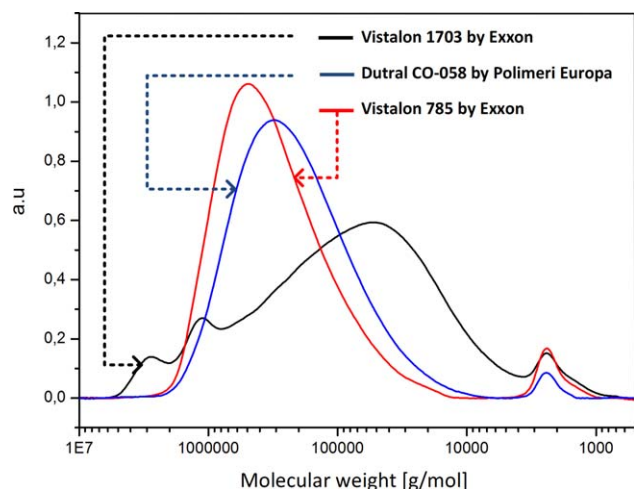


Figure 1. Molecular weight distribution of Vistalon 1703 compared with other two distributions of common industrial products. [Color figure can be viewed in the online issue, which is available at wileyonlinelibrary.com.]

(generally 1,4-Hesadiene, ENB, DCPD and VNB) is always made by peroxides.^{3–6}

While other typologies of insulation materials are diffused in practice and preferred to EPDM in some specific applications (mainly reduced insulation thickness), attention is focused in this article exclusively on EPDM, which remains one of the most diffused material for cables insulation,^{3,7,8}

The most important technical problems that providers are called to understand and to face is the wide scatter of the crosslinking density into final vulcanized items, from point to point inside the same cable and for different cables, especially for thick wall insulating.

Scattering is for sure the results of several concurring production variables that have to be carefully considered and controlled, as for instance items thickness, type of vulcanization ambient used (steam, nitrogen, etc.), temperature and curing time, curing agent type and concentration, composition of rubber, etc.

To put the research forward on this topic and to get final rubber based products passing high standard acceptability indices, in the present article the final results obtained by means of a wide experimental campaign conducted in cooperation with Mixer Spa and devoted to the combined analysis of the behavior during vulcanization and the mechanical performance of EPDM compounds vulcanized by peroxides are presented and critically discussed.

An industrial formulation is considered based on Exxon Vistalon 1703, a commercial ethylene, propylene and VNB terpolymer with wide molecular weights distribution (as shown in Figure 1), good processability and suitable for the extrusion of medium-high voltage electric cables. The special feature of this rubber compound analyzed is that uncured rubber is produced in pellets, allowing absorption of the peroxide on the surface of each single element, satisfactory stocking stability

and the possibility to vulcanize directly the compound by other factories.

The experimental tests were performed on the same EPDM compound, vulcanized at three different temperatures, respectively equal to 160, 180, and 200°C, for which both rheometer curves on an oscillating disc device and stress–strain curves on vulcanized items (under the same curing conditions) were experimentally determined.

Three different curing agents were tested, the first and the second relying into commercial peroxides provided by Akzo, the latter being a mixture of three different peroxides with different activity in the range of vulcanization temperature inspected, allowing good ambient stability and reasonable overall crosslinking activity.⁹

To have an insight about the effect obtained by varying the concentration of peroxide used, the molar concentration (referred to 100 g of polymer, see Table I) was both reduced to –50% and increased up to 150%, with 50% steps, assuming as 0% the standard concentration initially considered. For instance, with reference to data reported in Table I and BC-FF peroxide, a +100% concentration indicates that 2.72 grams per 100 g of polymer were used.

Experimental results showed that the final mechanical properties of the vulcanized items (e.g., tensile strength) are sensibly affected both by curing temperature and peroxide concentration. Variations have been observed by changing also the type of curing agent.

The wide experimental campaign conducted and the subsequent data reduction was useful to obtain an *a priori* calculated mechanical property for final vulcanized items; elaborated data model allows to precisely determine the most important parameters influencing the crosslinking density of the vulcanized rubber, like temperature, time, type of peroxide used and its concentration.

By means of the obtained results, suitably post processed, the provider may choose the most convenient vulcanization

Table I. Experimental Data Set Analyzed, EPDM Composition in Grams

Polymer	
<div style="border-left: 1px solid black; border-right: 1px solid black; padding: 5px;"> VISTALON 1703P Ethylene in wt. % 76.2 VNB-vinylnorbornene in wt. % 0.9 Mooney ML (1+4) 100°C 35.3 Manufacturer (Exxon) </div>	100
Silane-treated calcinated kaolin	55.5
Antioxidants	14.8
LDPE Riblene MR 10 MFI = 18.7 (ASTM D1238)	11.1
PE WAX	1.8
Peroxide M3 ^(†)	1.1
Peroxide BC-FF ^(†)	1.36
Peroxide 14-S ^(†)	0.85
^(†) peroxides are used separately	

Table II. Characteristics of the Polymers Considered in Figure 1

Type of polymer	ML(1+4) Mooney viscosity		% Ethylene by w.	% VNB by w.	MWD molecular weight distribution (Fig. 1)
	100°C	125°C			
Vistalon 1703 by Exxon	-	25	77	0.9	Very broad
Vistalon 785 by Exxon	-	30	49.0	-	narrow
Dutral CO-058 by Polimeri Europa	80	-	52	-	narrow

conditions in order to guarantee a suitable level of vulcanization and crosslink homogeneity.

Finally, in order to theoretically interpret the experimental results, a kinetic model of peroxide decomposition is presented in the article, considering the complex set of reactions involved in peroxide crosslinking: namely, homolytic cleavage of peroxide, hydrogen abstraction, polymer radicals formation, polymer radicals coupling, crosslink formation, and polymer scission. In the case of EPDM, the amount and type of the third-monomer, could be considered, but in a first approximation it is not accounted for when dealing with EPDMs with lower concentrations of the third-monomer.

Conversely, in the presented crosslink scheme, the different activity from alkyl and oxy radicals in the homolytic cleavage of peroxide and the secondary reactions as oxygenation and acid-catalyzed decomposition of peroxide may be well reproduced. After some tedious algebra on the first order differential equations coming from the chemical scheme, a single second order non homogeneous and non linear differential equation is obtained, allowing after best fitting on experimental rheometer curves, to determine the partial kinetic constants influencing the vulcanization process and hence giving quantitative information on the activity of the single peroxides and the mixture.

Thanks to the numerical model with parameters tuned through the present experimentation, it is possible the prediction, with simple computer simulations, of (1) the optimal curing time and temperature^{10–15} and (2) the most suitable peroxide to be used in order to maximize the final crosslinking density of an item with given geometry.¹⁶

Finally, it is possible to compare (at least for single peroxides) partial reaction constants provided by the model with those estimated by peroxide producers, to put in evidence both the accuracy and the limits of applicability of a simplified approach based on Arrhenius's law and widespread in common practice.

EXPERIMENTAL PART

The polymer used is a commercial EPDM, with properties furnished by the provider summarized in Table II. In the same table, other two commercial products are considered for a comparison.

A preliminary characterization of the molecular weight distribution was conducted in the laboratory and results are reported in Figure 1. Polymer molecular weights are measured from both conventional GPC using a differential refractive index detector (DRI) and low angle laser light scattering (LALLS) detector.

Molecular weight is reported in the horizontal axis (logarithmic scale), whereas the vertical axis is the normalized differential weight fraction in arbitrary units (a.u.). It is interesting to notice that the area bounded by the curve, x -axis and a fixed molecular weight, say M_{w0} , previously divided by the total area under the curve represents the probability to find molecular weights lower than M_{w0} . As can be seen from a critical comparison among all curves, Vistalon 1703 distribution is somewhat wider than other common products available in the market stock.

Available data regarding the other row materials used to produce the EPDM compound are the following:

- Silane-treated calcinated kaolin is Polarite 503S provided by Imerys.
- LDPE (low density polyethylene) is Riblene MR10 supplied by Polimeri Europa (density 0.918, melt flow rate 190°C/2.16 kg 20 g/10 min).
- PE Wax is Polyethylene A-C 617A provided by Honeywell (drop point 101°C).
- the antioxidant is polymerized 2,2,4-trimethyl-1,2-dihydroquinoline (TMQ) provided by LANXESS.

The EPDM compound was industrially produced and its composition is summarized in Table I.

Three different curing agents were investigated for the EPDM compound. The first, hereafter called M3 for the sake of clearness, is a mixture and it is produced by Mixer Spa. The three peroxides composing the mixture are the following: Trigonox T, Perkadox BC-FF, and Perkadox 14S. Mixture M3 is constituted by two commercial peroxides with the same thermal decomposition constants, see Table IV. The reason at the base of the utilization of a mixture having two peroxides with, in practice, the same kinetic constants is mainly technological and is aimed at obtaining a liquid mixture suitable for absorption on pellets surface. The mixture ratio of BC-FF, 14S-FF, and Trigonox T is respectively, 35–15–50% by weight.

The second and third peroxides investigated are commercial products provided by AkzoNobel,¹⁷ having commercial names as Perkadox BC-FF and Perkadox 14S-FL. They will be indicated in the following comparisons as BC-FF and 14-S for the sake of conciseness. Perkadox BC-FF is dycumil peroxide whereas Perkadox 14S-FL is a di(*tert*-butylperoxyisopropyl) benzene. They exhibit a half time equal to 1 h at 138 and 146°C, respectively, see Table IV. The peroxides are therefore quite similar; nonetheless, some perceivable differences in the experimental rheometer curves of the EPDM under consideration were observed.

Table III. Standard Concentrations of the Curing Agents Corresponding to 5.037 mmol per 100 g Polymer

Peroxide M3	1.10
Peroxide BC-FF	1.36
Peroxide 14-S	0.85

The curing agents were added to the EPDM compound by using a laboratory twin-roll mixer at the temperature of 85°C. When the compound melted, the peroxide was added and then the blend was mixed for 10 min.

The amount of peroxide, referred to 100 g of polymer is variable. In particular, during experimentation, three different peroxides (or mixture of peroxides) at five different concentrations were utilized. At a fixed concentration, the same molar concentration was utilized for each peroxide, taking into account the actual activity of each peroxide. One of the peroxides considered, indeed, is a biperioxide. Therefore, its activity is twice the activity of the others and, consequently, the molar concentration used was one half those of the mono-peroxides.

The chosen standard concentration, labeled as “±0%”, is equal to 5.037 mmoles per 100 g of polymer for each peroxide and it corresponds to the weight percentages of the different peroxides reported in Table III. It was considered as “standard” because this concentration is now commonly used in the industrial production process.

Four additional concentrations were tested, called −50%, +50%, +100%, and +150% for the sake of clearness. Labels indicate the molar concentration of the curing agent with respect to the standard concentration. For instance, a +50% concentration indicates that 1.5 moles with respect to the standard one were used.

Several experimental tests were conducted by the authors on the obtained EPDM rubber compounds. The experimentation was conducted varying the following parameters:

1. Curing agent: two different peroxides and a mixture were tested on the compound.
2. Concentration of the curing agent: five different concentrations for the different curing agents investigated were considered.
3. Vulcanization temperature: three different temperatures were used.

Table IV. Half-life Temperatures of the Peroxides Analyzed at 0.1, 1, and 10 h

Peroxide typology	$t_{1/2}$ in h	0.1	1	10
TRIGONOX T		169	146	117
PERKADOX BC-FF		162	138	112
PERKADOX 14 S-FL		169	146	117

TRIGONOX T: ter-butylcumylperoxide.

PERKADOX BC-FF: dicumyl peroxide.

PERKADOX 14S-FF: di(tert-butylperoxyisopropyl) benzene.

Curing agent M3 is a mixture of BC-FF, 14S-FF, and Trigonox T.

4. Although the direct experimental determination of crosslinking density would require DSC's, rheometer gives an indirect information on the state of cure, as extensively demonstrated by Sun and Isayev.¹⁸ The average $M(t)$ curves obtained may indeed be used to calculate the evolution of the vulcanisation degree $\alpha_{\text{exp}}(t)$ using Sun and Isayev¹⁸ relation:

$$\alpha_{\text{exp}}(t) = \frac{M(t) - M_{\text{min}T}}{M_{\text{max}T_0} - M_{\text{min}T_0}} \quad (1)$$

where:

- a. $M_{\text{min}T}$ is the minimum value of torque S' during a cure experiment at temperature T . Before reaching this minimum value, α_{exp} is considered equal to zero.
- b. $M_{\text{min}T_0}$ and $M_{\text{max}T_0}$ are the minimum and maximum torque values, obtained for a cure experiment at a temperature T_0 low enough to allow neglecting reversion. In this way, rheometer curves to fit always range between 0 and 1, with a maximum torque sensibly lower than 1 for high vulcanization temperatures.

Experimental results presented in this section are twofold: a thermal characterization to determine the state of cure of each sample conducted by means of a standard ODR (oscillating disc rheometer) and standard stress–strain uniaxial tests to mechanically characterize the cured specimens.

ODR test allows a macroscopic determination of the vulcanization characteristics of vulcanizable rubber compounds. Such method was here used to indirectly determine the rate of cure. It is essentially a measure of shear modulus of the fully cured rubber. The measurements were conducted in an oscillating disc curometer¹⁹ (GB3 Rheocheck).

Samples were prepared in agreement with ASTM D 1485 method, considering small cylindrical specimens with a diameter equal to 20 mm and a height equal to ~12.5 mm. Specimens were conditioned at constant room temperature equal to 25°C, as required by method ASTM D 2048. Tests were performed with a thermo-stated equipment that allowed a precise control of the design curing temperature. Three different temperatures were used, respectively equal to 160, 180, and 200°C. A wider range of temperatures was experimentally investigated by the authors, namely from 120°C up to 220°C, but the activity of the curing agents resulted suboptimal out of the range 160–200°C.

For each test, three replicates were considered, averaging rheometer curves among the three replicates.

Dealing with rheometer curves, three different temperatures for three curing agents were inspected, at five different concentrations. Three replicates for each vulcanization condition were considered within the experimental campaign, in order to reduce possible inaccuracies of the experimentation. In this manner, a total amount of 125 different rheometer curves were experimentally determined. Results presented refer to mean values obtained.

To evaluate if peroxide concentration, temperature and typology of curing agent result into different final mechanical properties of the vulcanized items, the same EPDM samples previously

vulcanized at the different temperatures and the curing agents concentrations were tested under uniaxial stress-strain conditions, in an universal testing machine (GB3 Tensorcheck), following ASTM D412²⁰ and ASTM D 1456-86.

The samples for mechanical test were hot-pressed under the pressure of 50 bar for a curing time equal to their t_{90} , deduced from the previously performed rheometer curves. The geometrical shape of the samples with standardized dimensions was in agreement with ASTM D 1456-86.

Stress-strain characterization was conducted up to failure under large deformations conditions, in order to evaluate tensile strength and elongation at failure of each cured sample.

As a result of the experimentation, a huge amount of data were collected and suitably post processed, including rheometer curves at different temperatures and stress strain curves of the vulcanized items.

Rheometer Curves

In figures from Figures 2–6, detailed comparisons among the performances during vulcanization (rheometer curves) exhibited by the three different curing agents at different concentrations are shown. These comparisons are useful to have an insight into the most suited curing agent to be used at different temperatures.

From a detailed analysis of rheometer results, the following aspects are worth noting:

1. For a temperature equal to 160°C, all curing agents inspected are underperforming, reaching asymptotically the maximum torque at excessively large vulcanization times, far away from the limit of acceptability for an industrial efficiency.
2. Comparing the maximum torque reached at different temperatures, it is worth noting that all vulcanization agents perform better at 200°C, with a torque generally higher than those reached at 180 and 160°C.
3. M3 curing agent underperforms at low concentrations (especially at -50%), whereas a concentration increase results into quite beneficial effects, compare for instance Figures 6 and 2. Considering the half-life temperature of peroxides reported in Table IV, it is expected that the behavior in kinetic terms of M3 mixture is intermediate between BC-FF and 14-S, since Trigonox T is essentially equivalent (from a kinetic point of view) to Perkadox BC-FF. The intermediate behavior may be appreciated only for +150% concentrations, where, after the scorch point up to the plateau is reached, the M3 rheometer curve is strictly bounded by BC-FF and 14-S ones.
4. For +150% concentrations and for a curing temperature equal to 200°C, it can be observed that the maximum torque provided by all curing agents (M3, BC-FF, and 14-S) is roughly the same (around 55 dNm, see Figure 6). Furthermore, the times needed to obtain 90% of the maximum torque (t_{90} values) seem very similar, meaning that also the kinetic constants at 200°C should be very similar.
5. As expected, in all cases, experimental rheometer curves do not exhibit perceivable reversion, due to the low amount of unsaturated bonds present in the EPDM utilized.

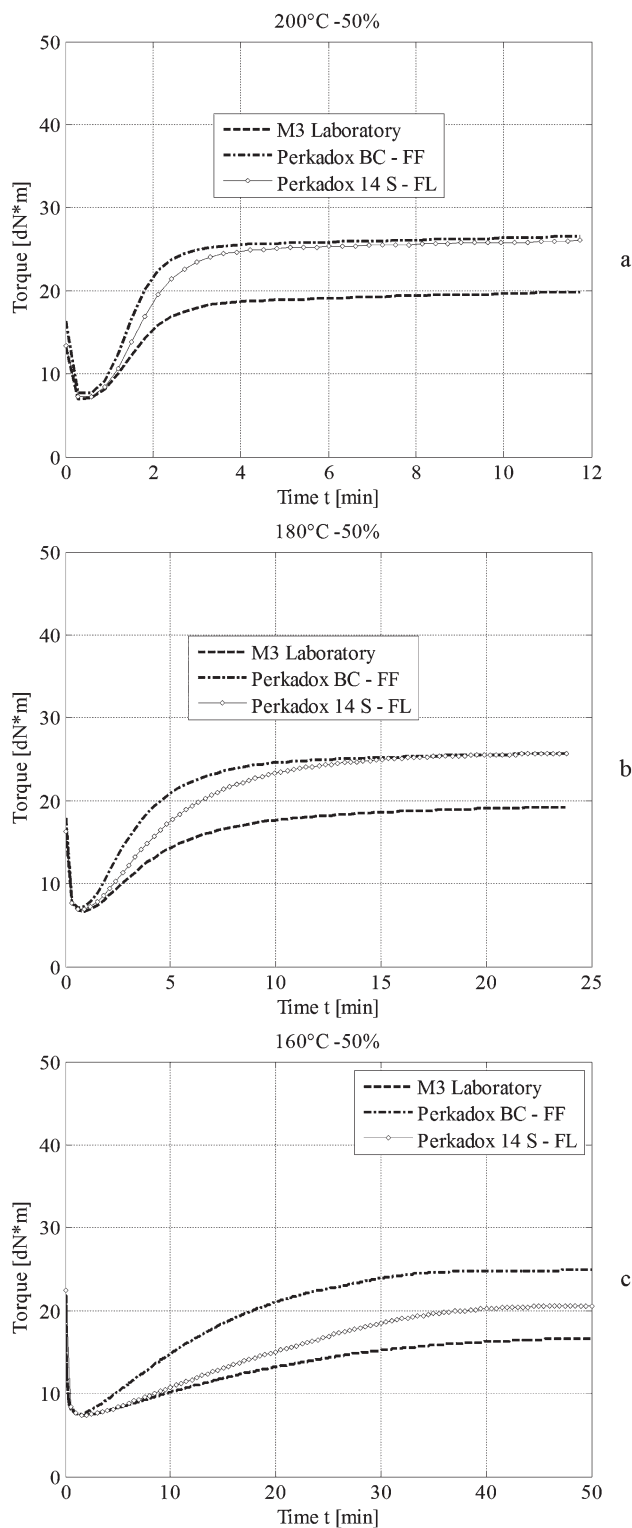


Figure 2. Experimental torque curves at -50% concentrations. a: 200°C, b: 180°C, c: 160°C.

From our experience, we would conclude that the optimal behavior for all curing agents may be obtained at 150% concentrations. Such a deduction is supported by figures from Figures 7–9, where rheometer curves obtained at different concentrations are normalized to 1 using Sun and Isayev procedure¹⁸ and directly compared.

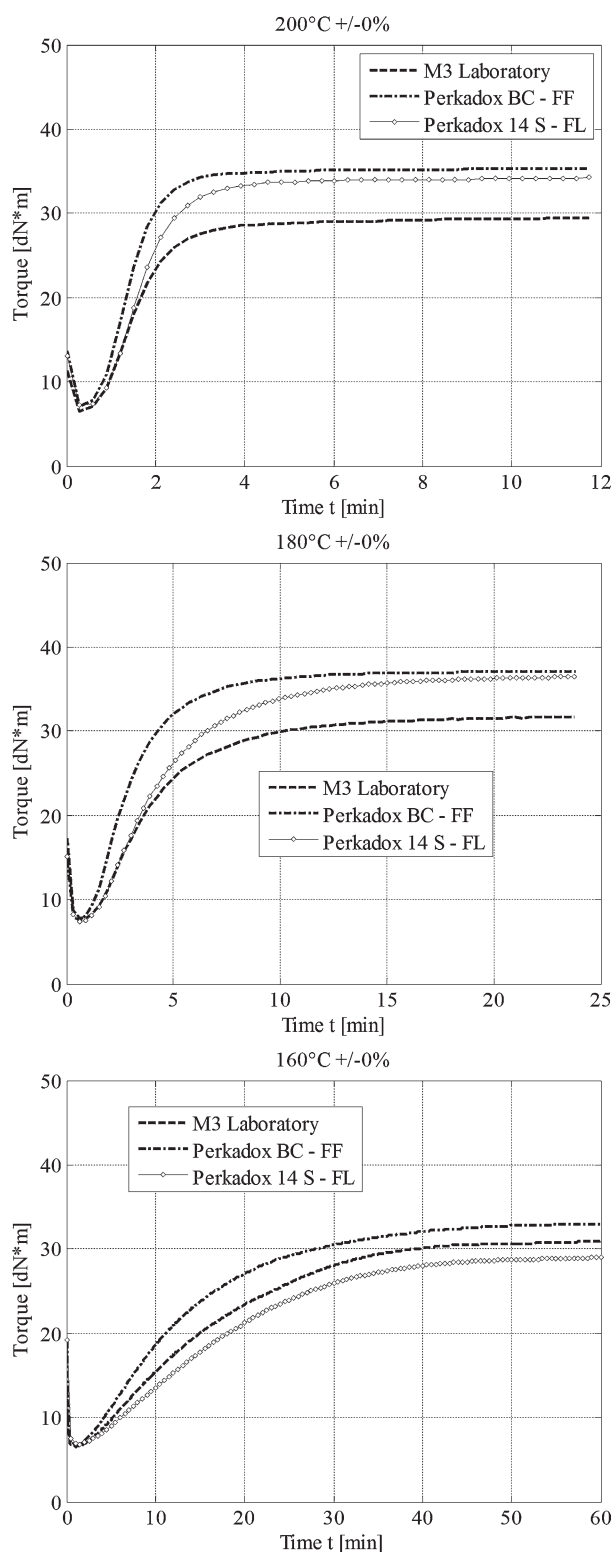


Figure 3. Experimental torque curves at $\pm 0\%$ concentrations. a: 200°C, b: 180°C, c: 160°C.

From a practical point of view, since no reversion is present for all the cases analyzed and minimum and maximum values of the torque at the three temperatures are very similar, normalization in practice reduces in dividing each value of the torque by

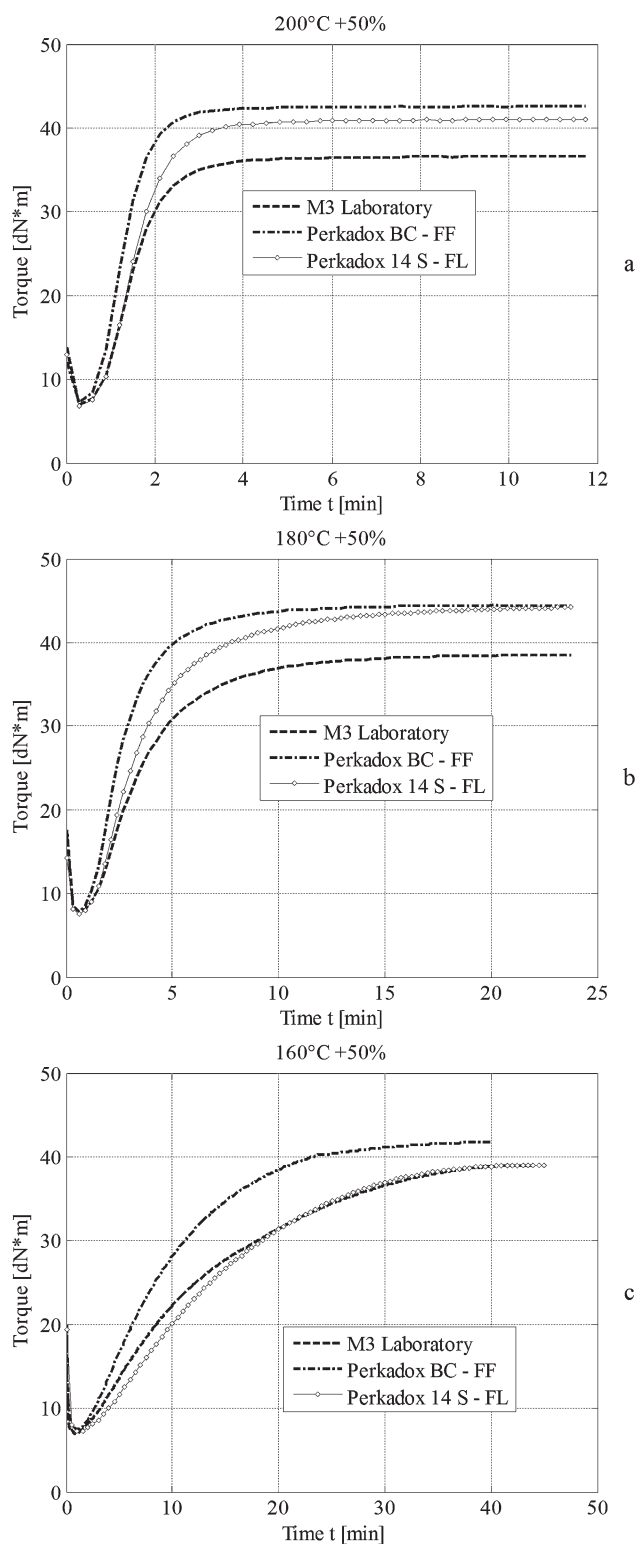
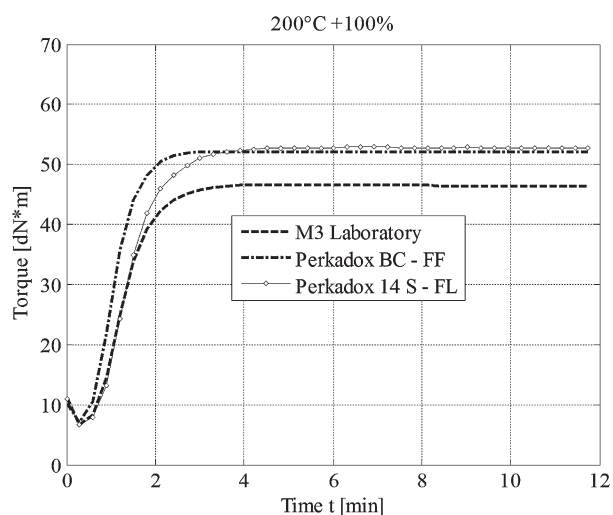
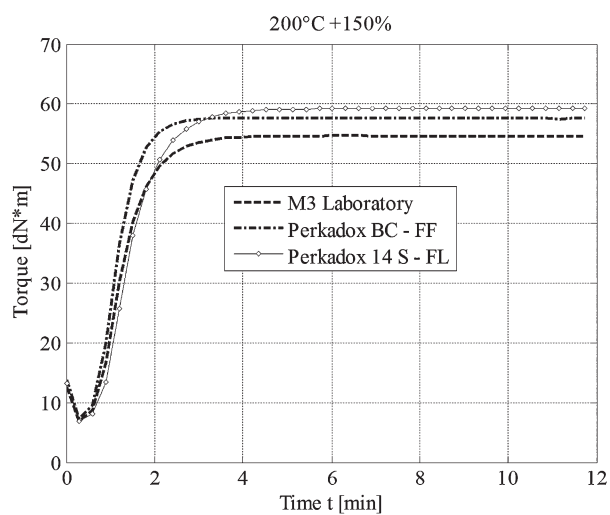


Figure 4. Experimental torque curves at $+50\%$ concentrations. a: 200°C, b: 180°C, c: 160°C.

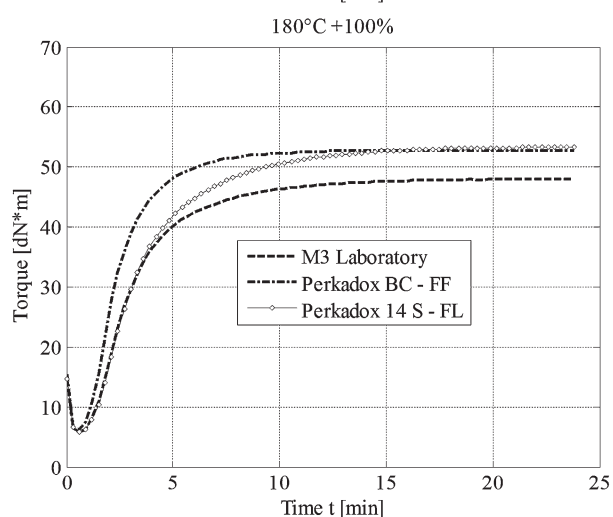
the maximum torque,^{15,21,22} which occurs at the end of the test. The different curves represented refer to the different concentrations explored in the experimental campaign, namely -50% , $\pm 0\%$, $+50\%$, $+100\%$, $+150\%$.



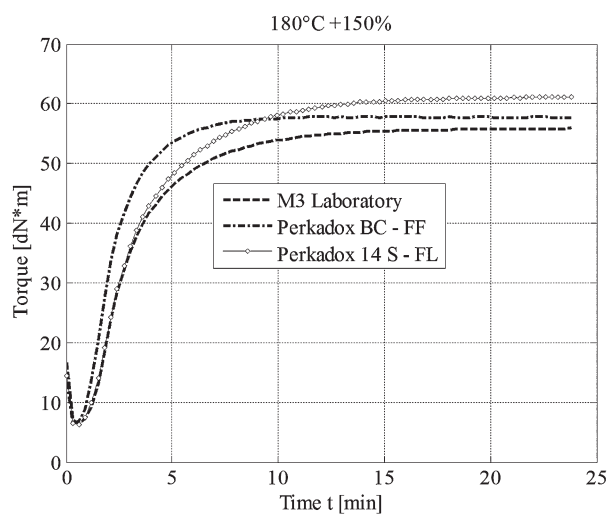
a



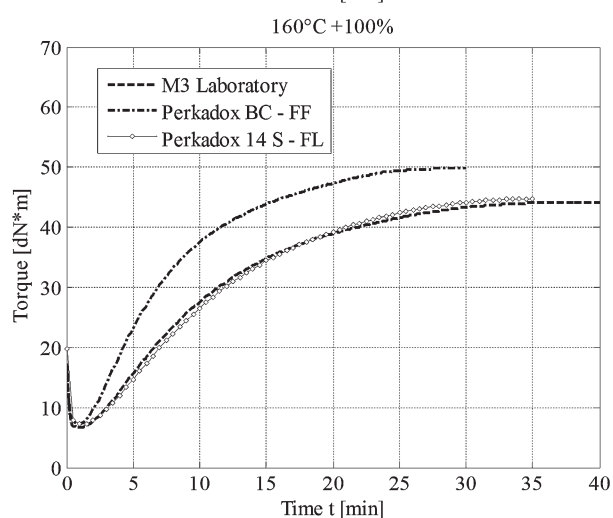
a



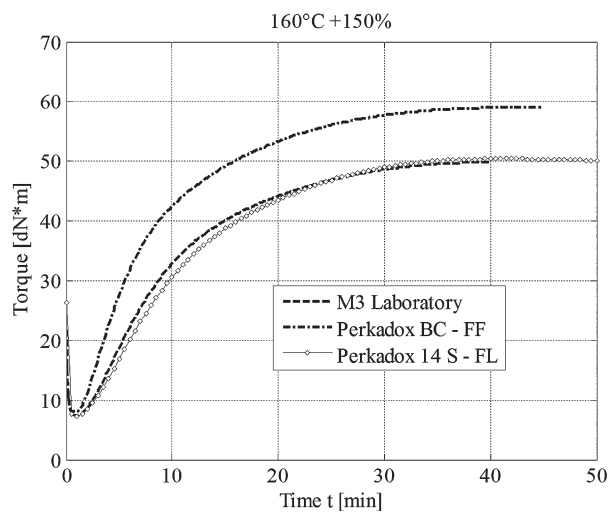
b



b



c



c

Figure 5. Experimental torque curves at 100% concentrations. a: 200°C, b: 180°C, c: 160°C.

Figure 6. Experimental torque curves at 150% concentrations. a: 200°C, b: 180°C, c: 160°C.

Figure 7 refers to M3 mixture, Figure 8 to BC-FF and Figure 9 to 14-S, respectively. Subfigures a, b, and c refer to curing temperatures equal to 160, 180, and 200°C, respectively.

As it is possible to notice, rheometer curves tend asymptotically to that corresponding to a concentration equal to 150%, meaning that a further increase into peroxide concentration would not result into an increase of final crosslinking density, being thus useless in practice.

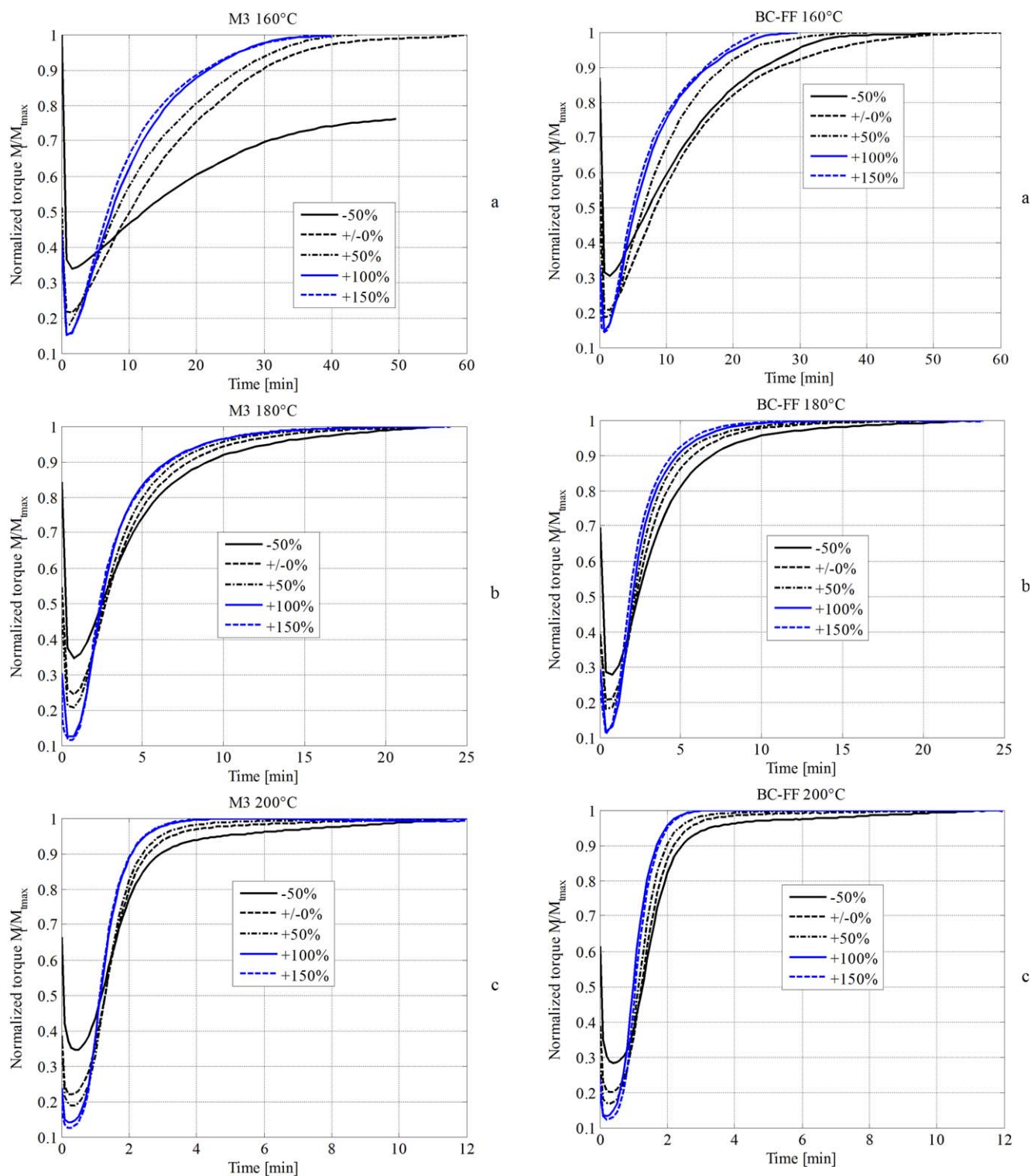


Figure 7. M3 peroxide mixture. Normalized experimental rheometer curves at different peroxide concentrations. a: 160°C, b: 180°C, c: 200°C. [Color figure can be viewed in the online issue, which is available at wileyonlinelibrary.com.]

In Figure 10, a direct comparison among rheometer curves at +150% obtained using BC-FF, 14-S and M3 at three vulcanization temperatures (a: 160°C, b: 180°C, and c: 200°C)

Figure 8. BC-FF peroxide. Normalized experimental rheometer curves at different peroxide concentrations. a: 160°C, b: 180°C, c: 200°C. [Color figure can be viewed in the online issue, which is available at wileyonlinelibrary.com.]

is reported. As we can see, for a vulcanization temperature of 200°C, vulcanization curves are almost superimposable, meaning that for high curing agent concentrations and high

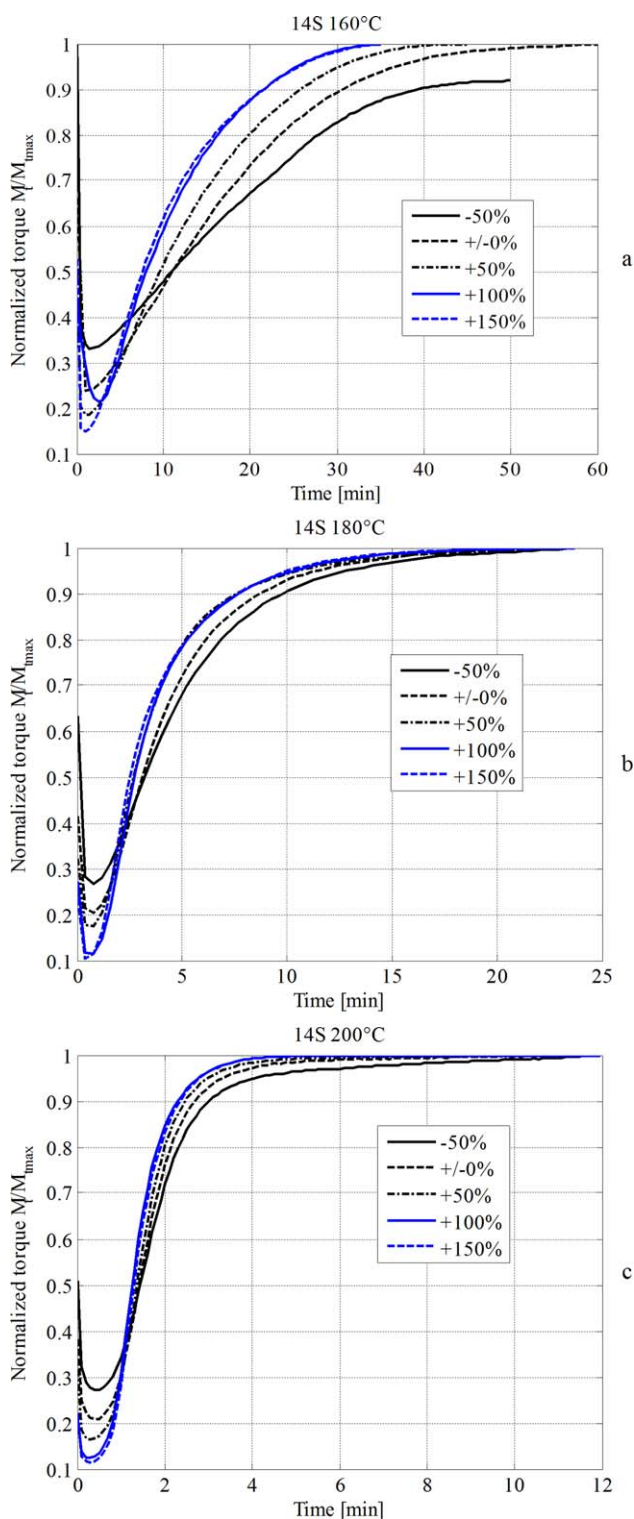


Figure 9. 14-S peroxide. Normalized experimental rheometer curves at different peroxide concentrations. a: 160°C, b: 180°C, c: 200°C. [Color figure can be viewed in the online issue, which is available at wileyonlinelibrary.com.]

vulcanization temperatures, the type of curing agent used has, in practice, no effect on the degree of induced crosslinking.

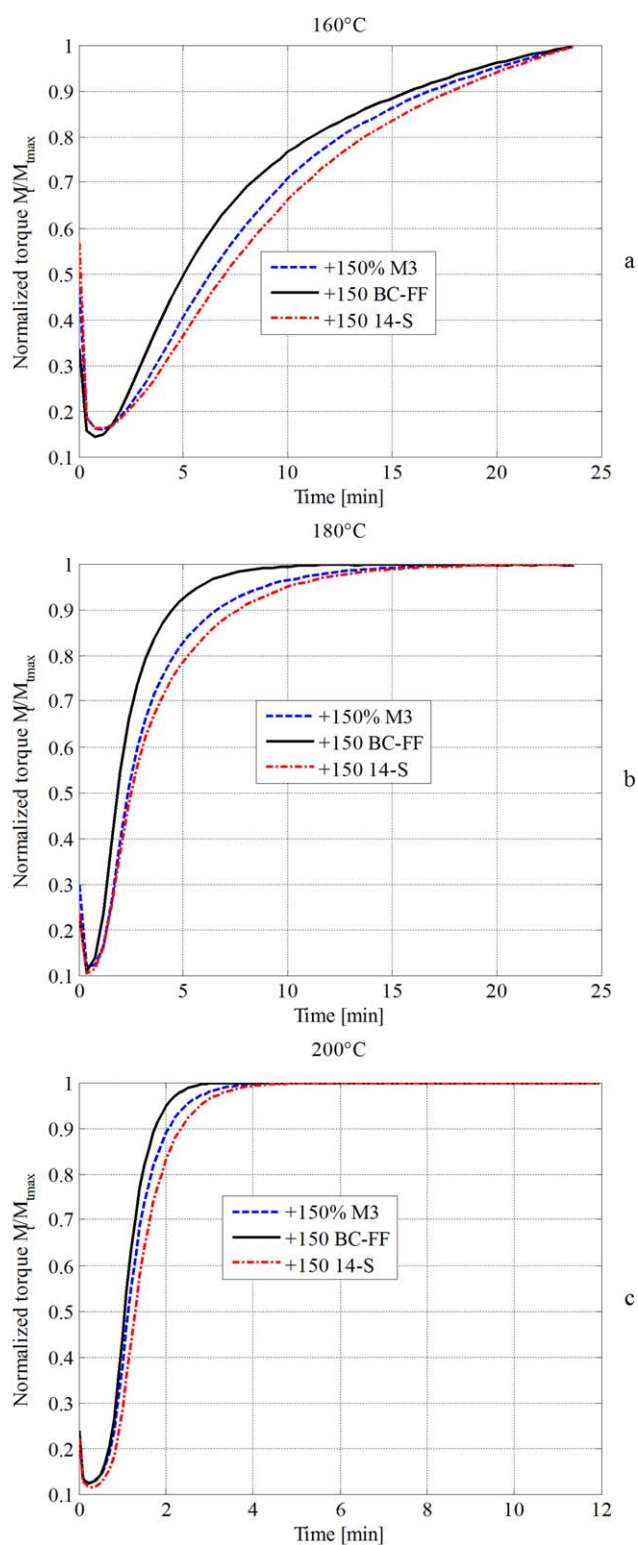


Figure 10. Comparison among rheometer curves obtained at +150% with M3, BC-FF, 14-S. a: 160°C, b: 180°C, c: 200°C. [Color figure can be viewed in the online issue, which is available at wileyonlinelibrary.com.]

Furthermore, from Figure 7, 8 and 9, it is particularly clear that increasing curing agent concentration, reticulation exhibits an asymptotic behavior, in all analyzed cases. As a matter of fact,

rheometer curves corresponding to +100% and +150% are in practice superimposable, meaning that, beyond these concentrations, the reticulation is fully independent on the curing agent concentration. Experimental evidences show that optimal cross-linking could be obtained with at least double amount of peroxide in comparison to the standard one (100% concentrations), implicitly stating that the standard $\pm 0\%$ peroxide concentrations provides suboptimal vulcanized items.

Finally, to further support the conclusion that the curing behavior of M3 mixture is intermediate between BC-FF and 14-S, let us consider again normalized curves with peroxide concentration equal to 150% obtained with M3, BC-FF and 14-S depicted in Figure 10 at the three different temperatures, i.e., 160°C (a), 180°C (b), and 200°C (c). As expected, M3 curing curve exhibits an intermediate behavior between the two commercial peroxides. In particular, the crosslinking activity of BC-FF peroxide is the greatest one, 14-S exhibits the lowest kinetic velocity, whereas M3 mixture has an intermediate behavior, for all the selected curing temperatures. It is therefore expected that the kinetic constants associated to M3 within any numerical kinetic model stand between those found for BC-FF and 14-S.

Mechanical Properties of the Vulcanized Samples

All samples vulcanized in the rheometer chamber at the three different temperatures discussed (160, 180, and 200°C) and with the five peroxide concentrations inspected (50, 0, 50, 100, 150%) were subsequently mechanically tested in a universal testing machine, in order to determine cured rubber tensile strength.

As already pointed out, the working parameters for the preparation of the samples to test mechanically are the following: cure time equal to t_{90} deduced from the previously performed rheometer curves and geometrical shape of the samples with standardized dimensions, taken in agreement with ASTM D 1456-86. To this aim, full stress-strain curves were obtained under large deformation conditions up to failure. The typical stress-strain curve obtained for one of the samples is shown in Figure 11. Similar results are obtained for the other cases inspected and are not reported here for the sake of conciseness.

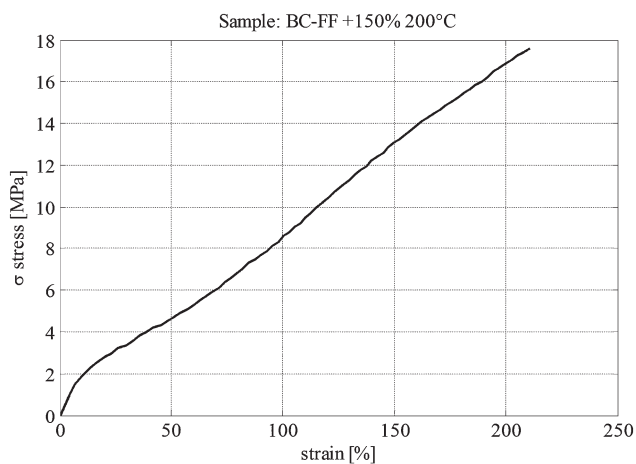


Figure 11. Typical stress–strain curve obtained experimentally on a vulcanized sample.

Apart tensile strength, a full stress-strain characterization allows the determination of other key mechanical parameters, e.g., deformation at failure, 100% modulus, etc.

Despite the wide number of properties that can be considered, we chose to consider as meaningful output mechanical parameter only tensile strength, because a nonlinear and sometimes nonmonotonic relationship between maximum torque and tensile strength²³ is possible.

As literature demonstrates, there is a concentration threshold for the peroxide representing a sort of upper bound, that, if exceeded, does not allow a further increase of the crosslinking density of the vulcanized item. This value has to be determined by producers, because the utilization of lower concentrations will result into suboptimal vulcanization quality. On the opposite, the presence of larger amounts of curing agent will not be particularly beneficial in terms of improvement of crosslinking density, leading to useless economic expenses. From present experimental results, considering preliminarily only the rheometer curves, it appears that the standard concentration (0%) is slightly suboptimal, leading however to results in terms of

Table V. Tensile Strength/Torque Experimental Values [MPa]/[dNm] for the Three Curing Agents Studied at Different Concentrations and Temperatures

Peroxide concentration	−50	±0	+50	+100	+150
M3	TS/TQ	TS/TQ	TS/TQ	TS/TQ	TS/TQ
200°C	8.0/20.3	12.3/29.7	14.0/36.8	14.4/46.7	15.6/54.7
180°C	8.3/19.9	13.6/31.9	14.0/38.7	15.1/48.1	16.2/55.9
160°C	7.4/14.9	12.0/25.7	12.5/29.8	14.4/41.2	14.4/46.5
BC-FF	TS/TQ	TS/TQ	TS/TQ	TS/TQ	TS/TQ
200°C	8.6/26.9	14.0/35.5	15.0/42.7	16.5/52.2	16.5/57.6
180°C	10.5/26.2	13.6/37.3	14.8/44.6	16.4/52.8	16.5/57.9
160°C	9.8/22.9	13.8/29.2	14.5/40.4	15.6/49.3	15.0/55.6
14S	TS/TQ	TS/TQ	TS/TQ	TS/TQ	TS/TQ
200°C	9.0/26.4	13.1/34.4	14.5/41.1	16.0/52.8	17.3/59.2
180°C	9.5/26.2	14.5/36.6	15.0/44.4	16.7/53.4	16.5/61.2
160°C	8.0/17.2	11.7/23.9	13.1/34.2	15.3/41.9	16.1/46.4

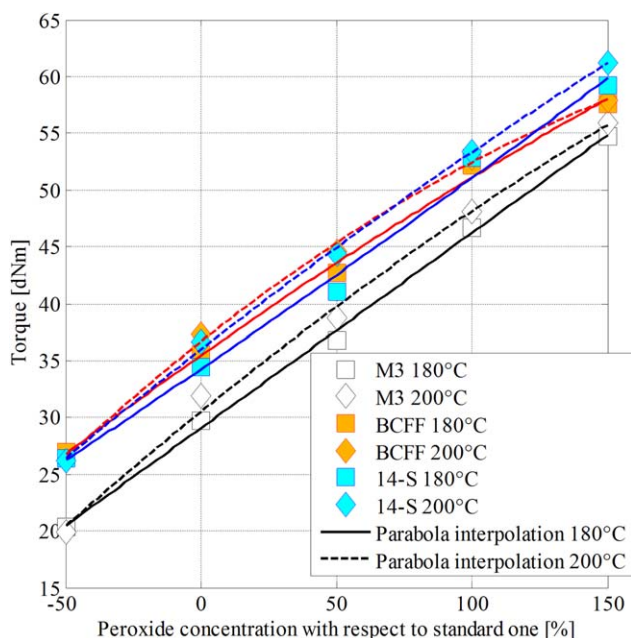


Figure 12. Peroxide concentration % versus torque. Experimental data (points) and parabolic numerical interpolation. [Color figure can be viewed in the online issue, which is available at wileyonlinelibrary.com.]

crosslinking density in any case quite satisfactory and near the maximum ones. In Table V, a synopsis of the average results obtained in terms of maximum torque and final tensile strength of three replicates is summarized.

To corroborate the idea that a greater concentration of peroxide with respect to the standard one results into an optimal crosslink of the EPDM under consideration, in figures from Figures 12–14 a synopsis of the mechanical experimental results available is represented in graphical form. In particular, in Figure 12, peroxide concentration (%) versus torque is represented for all the curing agents and temperatures investigated. Experimental data are repre-

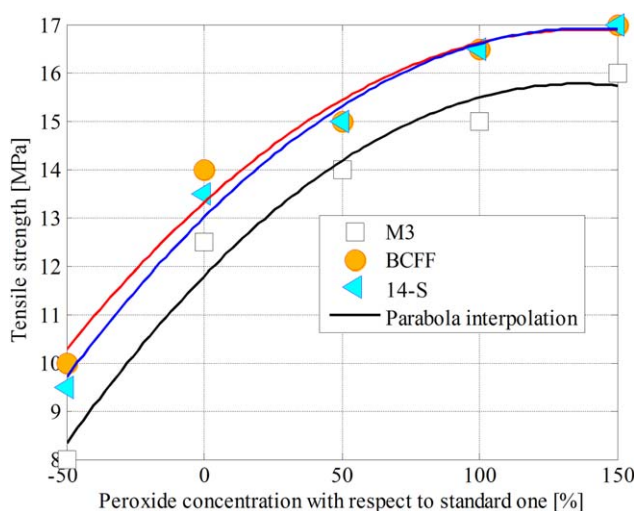


Figure 13. Peroxide concentration % versus tensile strength. Experimental data (points) and parabolic numerical interpolation. [Color figure can be viewed in the online issue, which is available at wileyonlinelibrary.com.]

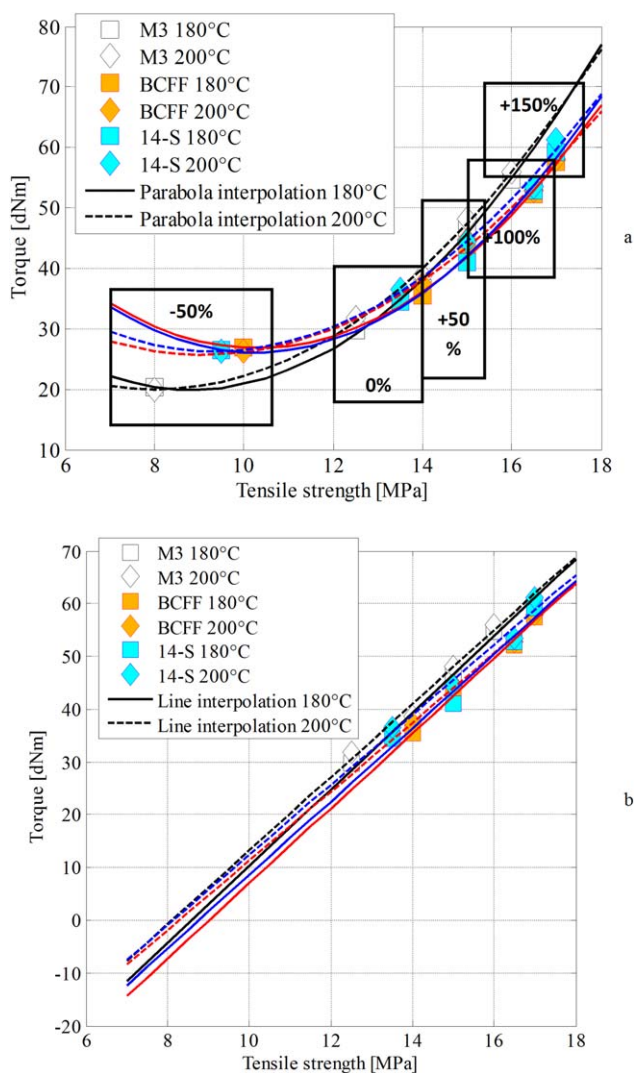


Figure 14. Tensile strength versus torque. a: Experimental data (points) and parabolic numerical interpolation. b: linear interpolation excluding -50% results. [Color figure can be viewed in the online issue, which is available at wileyonlinelibrary.com.]

sented with points (squares and diamonds refer to 180 and 200°C, respectively, white, orange and cyan colors to M3, BC-FF) whereas continuous (180°C) and dashed lines (200°C) are parabolic numerical interpolations. In Figure 13, the same symbols are utilized to represent the relationship between peroxide concentration and tensile strength, whereas in Figure 14 tensile strength versus torque is represented. It can be observed that tensile strength reaches an asymptotic value for 150% concentrations.

In Figure 15, the final tensile strengths as a function of peroxide concentration at three different temperatures are represented. Subfigures a, b, and c refer, respectively to M3 curing agent, Perkadox BC-FF, and Perkadox 14-S.

As can be noted, tensile strength increases as peroxide concentration increases. A plateau is generally reached in correspondence of $+150\%$ concentrations, again confirming that optimal concentration to use for this kind of EPDM is within the range $+100/+150\%$.

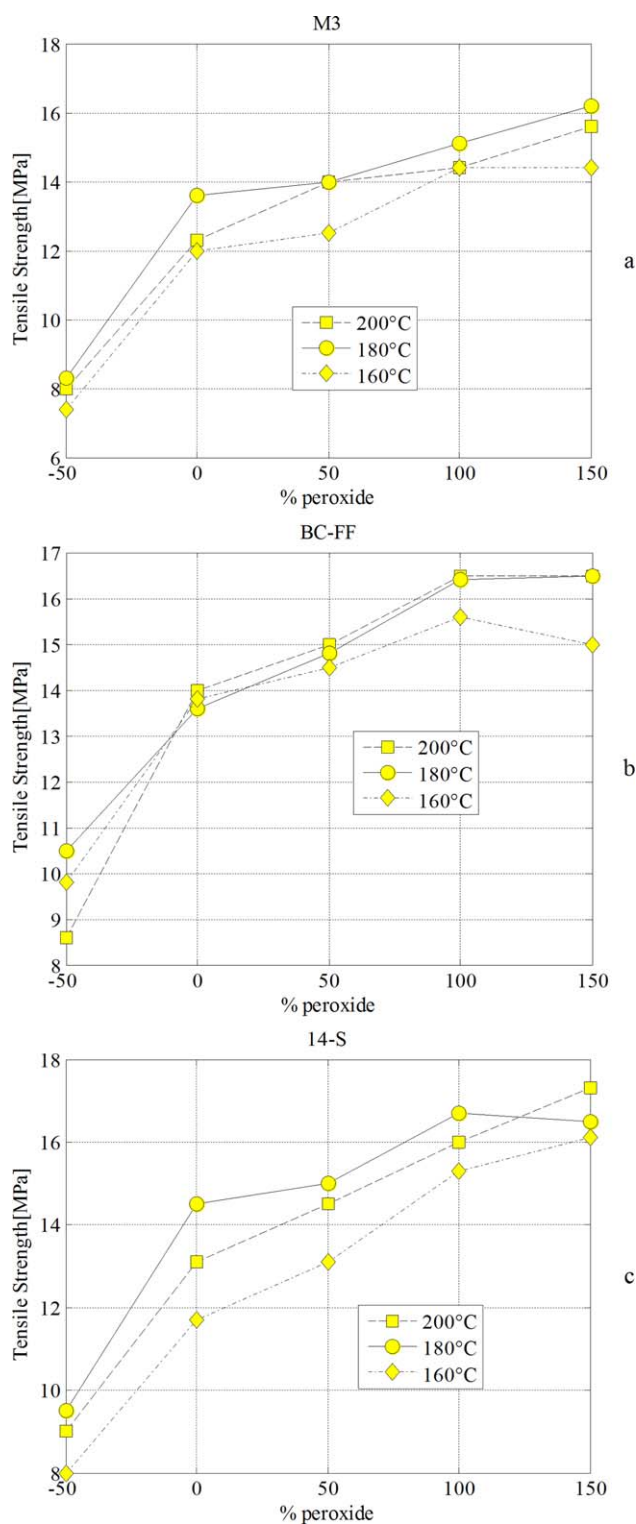


Figure 15. Tensile strength experimental results as a function of peroxide concentration. a: M3, b: BC-FF, c: 14-S. [Color figure can be viewed in the online issue, which is available at wileyonlinelibrary.com.]

In Figure 16 experimental tensile strength–maximum torque diagrams in correspondence of the three different curing temperatures analyzed are represented. Again, subfigures a, b, and c refer respectively to M3 curing agent, Perkadox BC-FF, and Perkadox 14-S.

Each curve is obviously constituted by five experimental points (one per concentration) and corresponds to a fixed vulcanization temperature, in such a way that square symbols refer to results at 200°C, circles to 180°C, and diamonds to 160°C.

As expected, curing obtained at 160°C provides, almost systematically, slightly lower values of maximum torque and tensile strength, whereas results at 180 and 200°C are experimentally superimposable. While results at 160°C are affected by a small scatter, it has to be emphasized both that they do not differ sensibly to results at higher temperatures and those tests at rheometer were stopped at 24 min before rheometer curves could clearly reach the plateau, i.e., before the crosslinking process ended. The results in Figure 16 confirm that torque–tensile strength curves do not depend sensibly on vulcanization temperature.

The torque–tensile strength relationship is generally nonlinear, but well approximates a straight line when results obtained with –50% concentrations are excluded. It has been established, indeed, that this concentration is clearly suboptimal and leads to an insufficient crosslinking degree.

To support this last hypothesis, in Figure 17 tensile strength as a function of the vulcanization temperature is represented. Each subfigure refers to different curing agent, so that “a” results are obtained with M3, “b” with Perkadox BC-FF, and “c” with Perkadox 14-S.

The five curves represented in each figure refer to the five curing agent concentrations investigated. As can be noted, values at –50% are sensibly lower when compared to those obtained with higher concentrations.

The remaining concentrations provide, from an experimental point of view, similar results, even some perceivable data scatters are still present at 0 and 50% concentrations. As expected, +150% concentrations are associated to generally higher tensile strengths when compared to those obtained with lower peroxide concentrations, when the results are compared at the same temperature, concentration and typology of peroxide. It is interesting to notice that tensile strength values at +100% and 150% are almost superimposable for all the cases analyzed, confirming once again that the optimal concentration of peroxide to be used falls in this range.

To have a comparative insight about relationships among tensile strength, torque and peroxide concentration at the different temperatures, in Figure 18 experimental results are depicted using a 3D representation. Peroxide concentrations, tensile strength and maximum torque are represented respectively on horizontal (x , y) and vertical (z) axes. Three different values per point are represented, one for each vulcanization temperature. Again square symbols refer to results at 200°C and diamonds to 160°C.

From the 3D representation, it is evident that (1) vulcanization temperature has little effect on the final vulcanized properties, (2) that at 150% concentrations the maximum tensile strength is reached and (3) that the relationship between torque and tensile strength does not deviate considerably from the linearity if results obtained for –50% concentrations are disregarded.

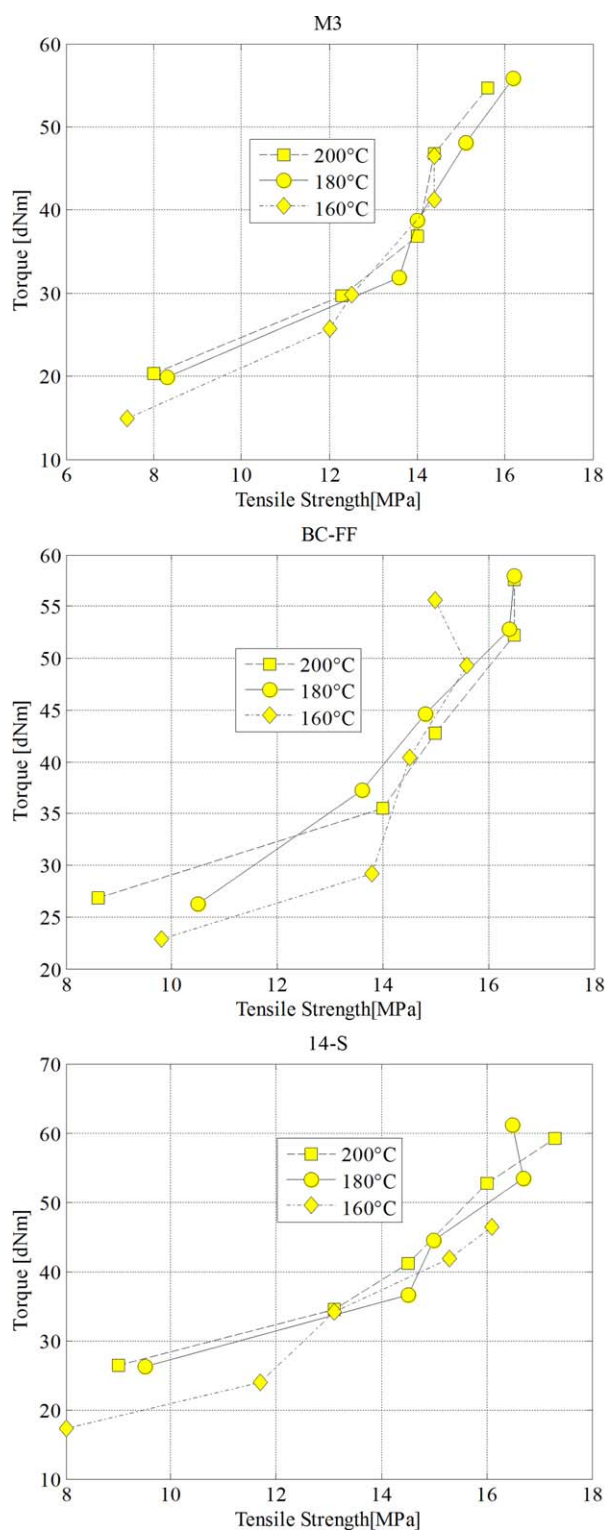


Figure 16. Experimental tensile strength-torque diagrams as a function of vulcanization temperature. a: M3, b: BC-FF, c: 14-S. [Color figure can be viewed in the online issue, which is available at wileyonlinelibrary.com.]

Linearity of the results can be appreciated well from the 2D results reported in Figure 14(b). Such a representation has a quite straightforward technical benefit, because allows an indirect evaluation of the tensile strength once the maximum torque

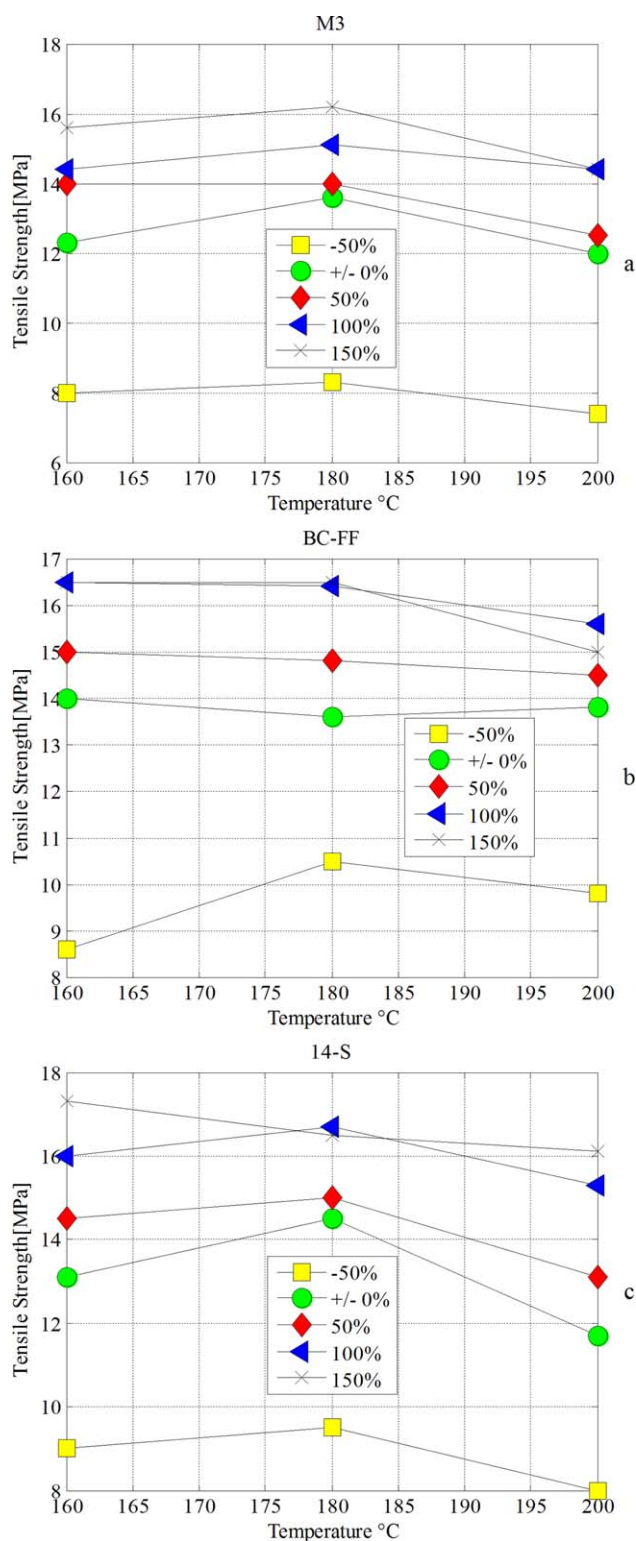


Figure 17. Tensile strength experimental results as a function of vulcanization temperature. a: M3, b: BC-FF, c: 14-S. [Color figure can be viewed in the online issue, which is available at wileyonlinelibrary.com.]

value is known. Furthermore, it simply correlates an *a priori* experimental evaluation (like that one obtained from the rheometer chart) with *a posteriori* mechanical characterizations performed on already vulcanized specimens.

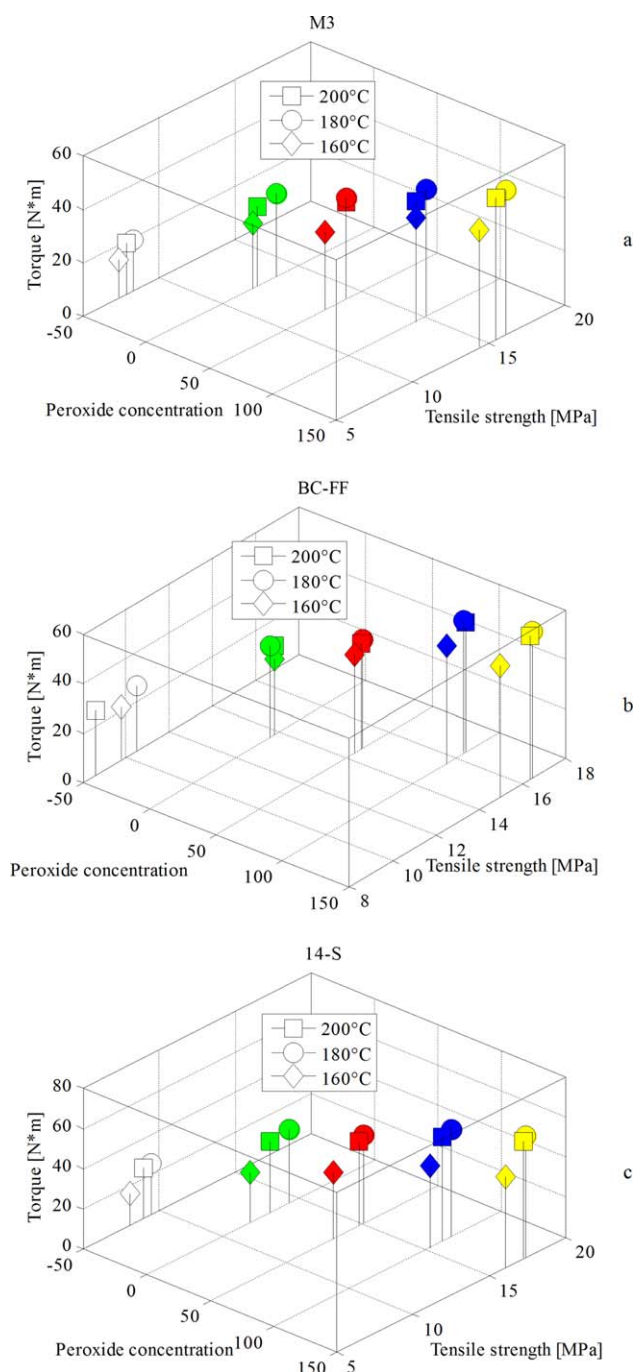


Figure 18. Experimental tensile strength-torque-% peroxide concentration diagrams as a function of vulcanization temperature. a: M3, b: BC-FF, c: 14-S. [Color figure can be viewed in the online issue, which is available at wileyonlinelibrary.com.]

Finally it is worth emphasizing that curing agents concentrations investigated in the present study are probably lower than those associated with an inversion of the behavior between tensile strength and maximum torque (or analogously final cross-linking density). As pointed out by Hoffmann,²⁴ indeed, a decrease of tensile strength may be experienced in correspondence of an increase of maximum torque for particularly large values of torque.

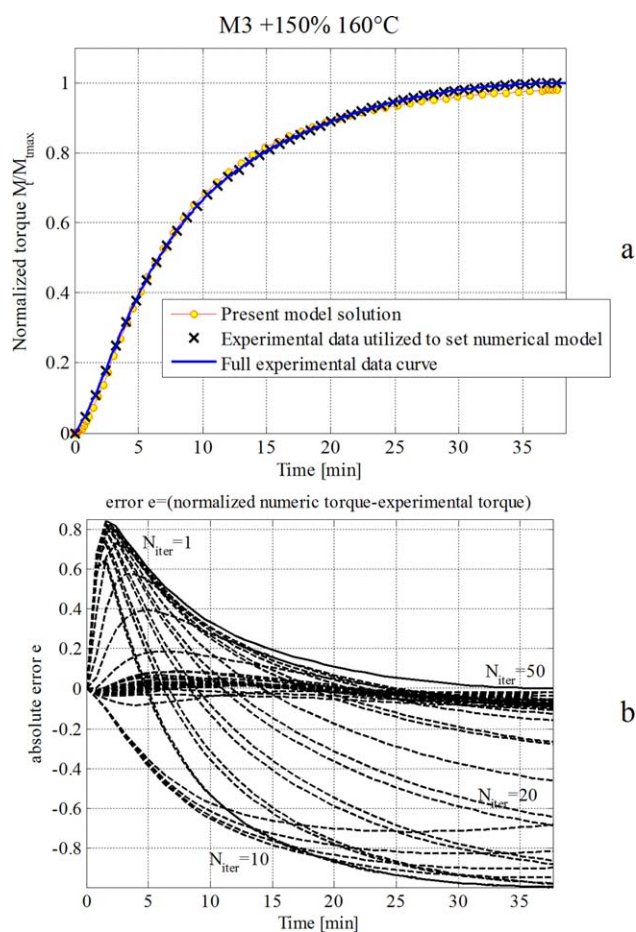


Figure 19. M3 curing agent, 160°C. Comparison between experimental data and numerical model. a: full normalized curve, b: difference between numerical model and experimental normalized torque at successive iterations. [Color figure can be viewed in the online issue, which is available at wileyonlinelibrary.com.]

NUMERICAL ASSESSMENT

A numerical assessment of the results obtained experimentally is provided in this section, after a brief description of the numerical model used to fit experimental data.

The model has kinetic bases, starts from the generally accepted reactions occurring in EPDM peroxide curing, translates chemical reactions into mathematical differential equations (set of first order ordinary differential equations, ODE system), manipulates the ODE system to reduce the problem to a single nonlinear ODE, solves the non linear equation through a standard numerical tool and provides an estimation of the kinetic constants entering into the model by means of standard least squares fitting of the experimental rheometer curves.

The approach proposed bases on the characterization of the curing process by means of partial reactions occurring in series and parallel and in their translation into mathematical differential relations constituting an ordinary differential equations system with many variables, which typically is solved resorting to numerical methods.

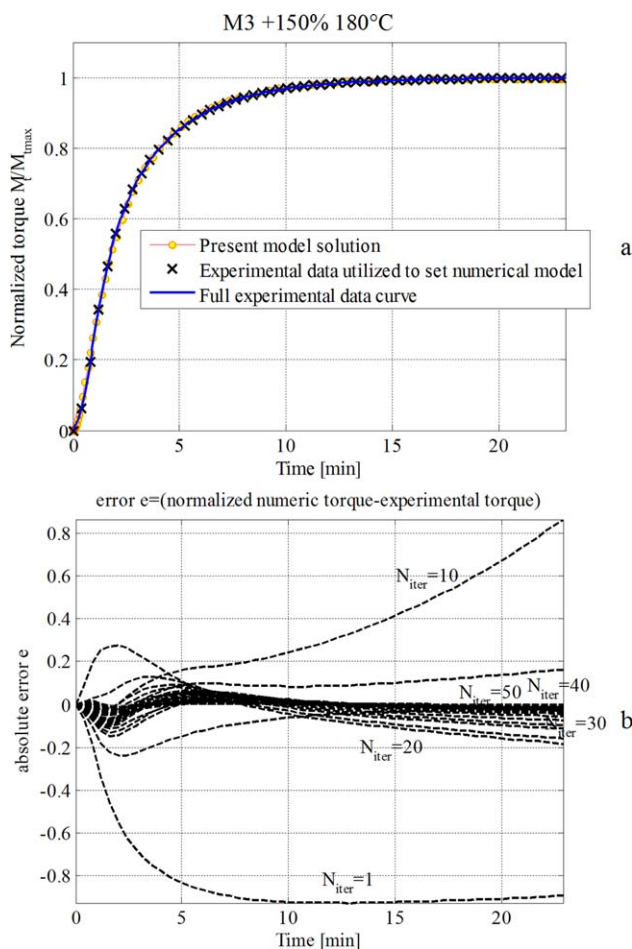


Figure 20. M3 curing agent, 180°C. Comparison between experimental data and numerical model. a: full normalized curve, b: difference between numerical model and experimental normalized torque at successive iterations. [Color figure can be viewed in the online issue, which is available at wileyonlinelibrary.com.]

The procedure, with some modifications *ad-hoc* implemented to adapt the model to the particular case study analyzed, belongs to a consolidated and robust family of numerical approaches that was already tested for the vulcanization with sulfur of both NR and EPDM and in presence of peroxides.^{15,16,22}

The main novelty and importance of the numerical procedure stands in the evaluation of kinetic constants for the peroxides mixtures, to be used in a successive phase to quantitatively determine the state of cure of high-medium voltage electric cables. The procedure, indeed, allows an indirect but reliable estimation of a single kinetic constant describing the whole vulcanization process. While such result is already at disposal to producers—typically derived by means of practical considerations following a first order single reaction scheme—for common commercial peroxides, it is unknown for the peroxides mixture at hand.

The basic chemistry in the generally accepted mechanism of peroxide cure of EPDM has been reviewed by van Duin

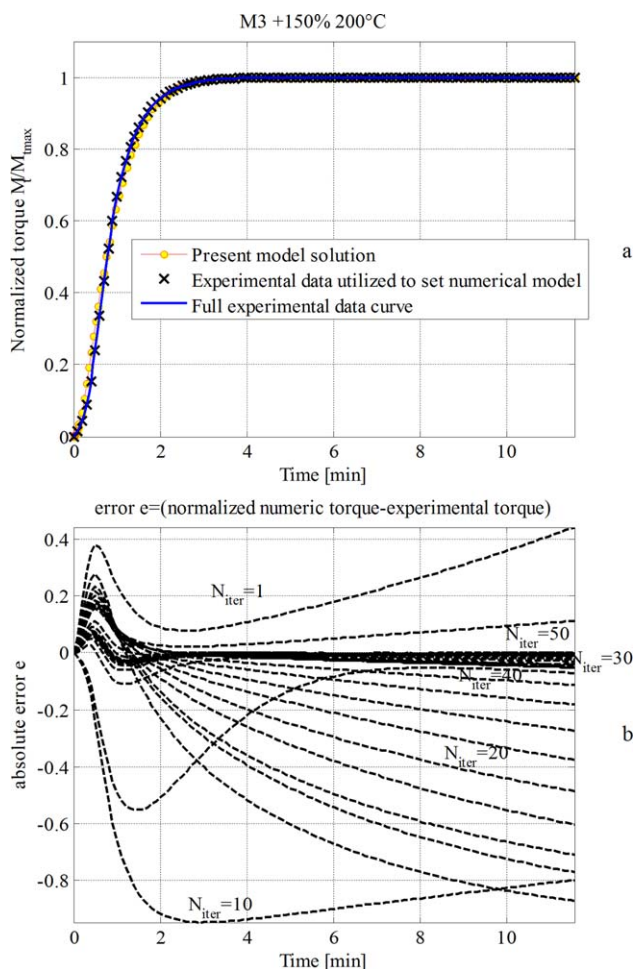
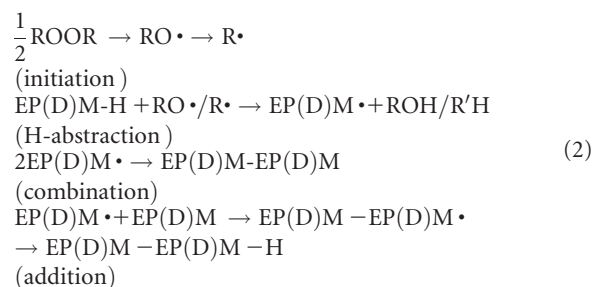


Figure 21. M3 curing agent, 200°C. Comparison between experimental data and numerical model. a: full normalized curve, b: difference between numerical model and experimental normalized torque at successive iterations. [Color figure can be viewed in the online issue, which is available at wileyonlinelibrary.com.]

and co-workers,^{25,26} and may be summarized by means of the following partial reactions occurring in series and parallel:



The chain of free-radical reactions is initiated by thermal decomposition of the peroxide, yielding primary alkoxy (RO•) or secondary alkyl radicals (R•). Subsequent abstraction of H-atoms from the EPDM polymer results in the formation of EPDM macro-radicals (EPDM•). Calculations based on kinetic

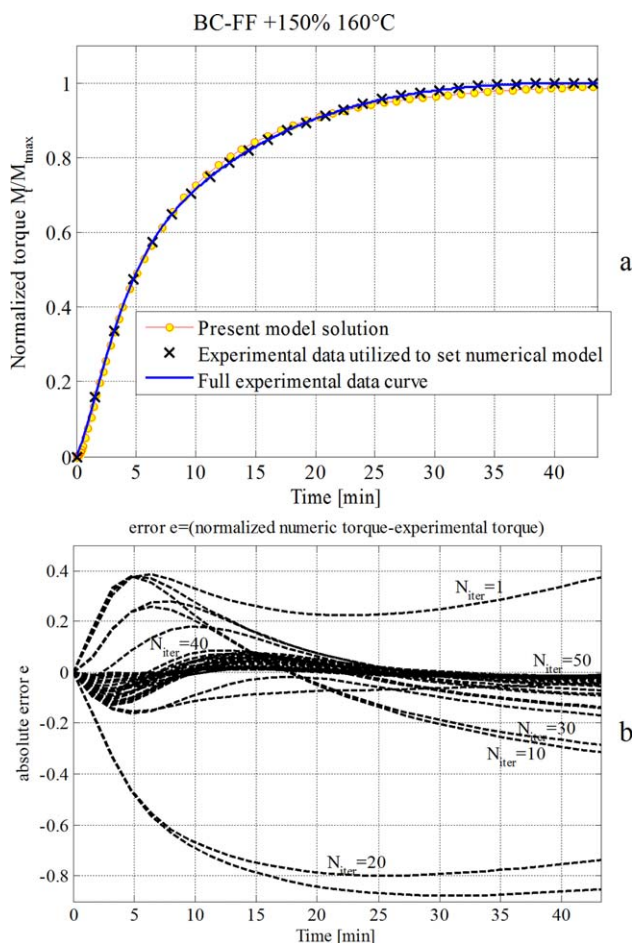


Figure 22. BC-FF curing agent, 160°C. Comparison between experimental data and numerical model. a: full normalized curve, b: difference between numerical model and experimental normalized torque. [Color figure can be viewed in the online issue, which is available at wileyonlinelibrary.com.]

data for H-abstraction indicate that H-abstraction mainly occurs along the saturated EPM polymer backbone,²⁶ whereas several electron paramagnetic resonance (EPR) spectroscopy studies have shown the selective formation of allyl radicals derived from the diene monomer.

Considering the energy required for the abstraction of the H-atoms within the formation of the back-bone, the allyl radicals are more probable than the others, because of the lowest energy required by the abstraction of the H-atoms.²⁷

The actual crosslinking proceeds via two pathways, which have been shown to be additive. Two EPDM macro-radicals either combine or, alternatively, a macro-radical adds to an EPDM unsaturation. Visible spectroscopy has confirmed the conversion of the EPDM unsaturation upon peroxide cure.²⁸ It is noted that in practical EPDM/peroxide compounds usually coagents, such as triallyl (iso)cyanurate, trimethylolpropane trimethacrylate or *m*-phenylenebis(maleimide), are included to increase the peroxide curing efficiency,^{24,29} which obviously affects the mechanism of peroxide cure.

In the numerical model, we have adopted for EPDM the kinetic scheme for the peroxide cross-link reactions summarized in eq.

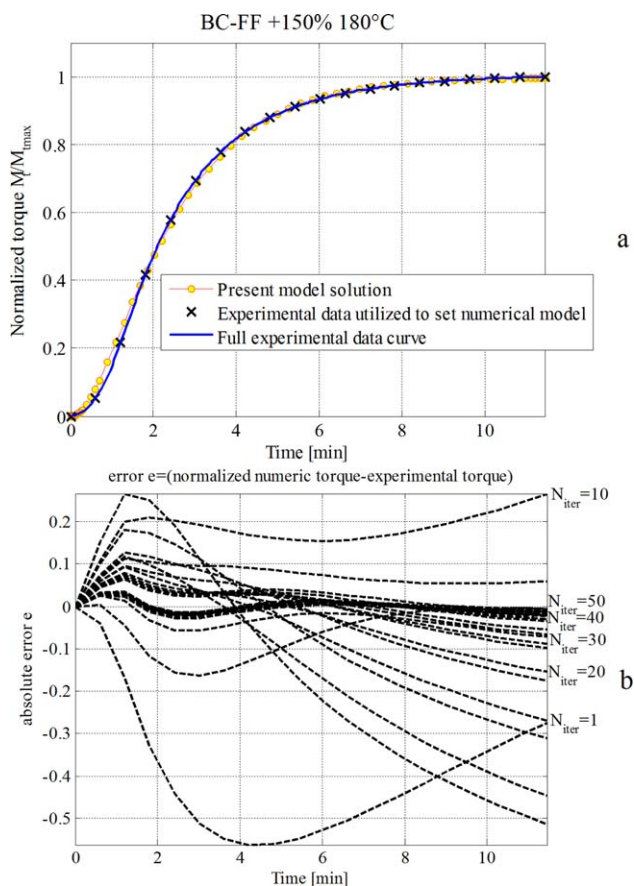
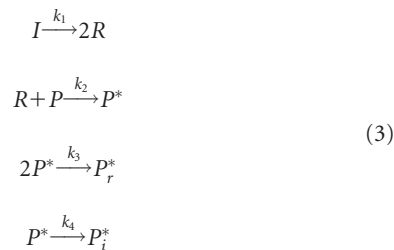


Figure 23. BC-FF curing agent, 180°C. Comparison between experimental data and numerical model. a: full normalized curve, b: difference between numerical model and experimental normalized torque. [Color figure can be viewed in the online issue, which is available at wileyonlinelibrary.com.]

(2), because it reproduces the most important steps occurring during peroxide curing, at the same time remaining sufficiently simple to handle.^{19,22}

Translating chemical reactions (2) into a more mathematical framework and focusing exclusively on EPDM rubber, the possible polymerization scheme to analyze may be the following:



In eq. (3), I is the peroxide, R the primary alkoxy ($\text{RO}\cdot$) or secondary alkyl radicals ($\text{R}\cdot$), P the uncured polymer, P^* is the EPDM macro-radical, P_r^* and P_i^* the matured cross-linked polymers, and $K_{1,\dots,4}$ are kinetic reaction constants. Here it is worth emphasizing that $K_{1,\dots,4}$ are temperature dependent quantities, hence they rigorously should be indicated as $K_{1,\dots,4}(T)$, where T is the absolute temperature. In what follows, for the sake of simplicity, the temperature dependence will be left out.

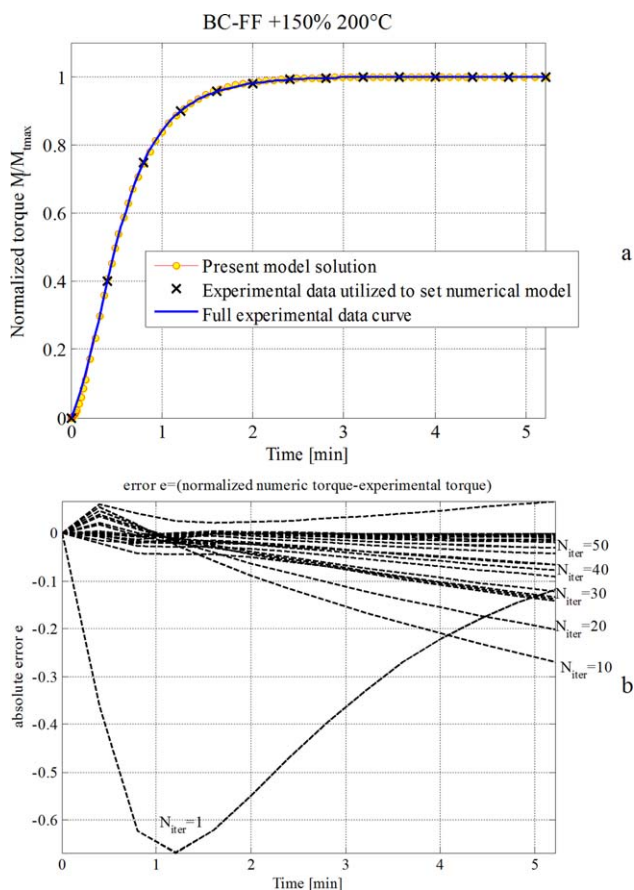


Figure 24. BC-FF curing agent, 200°C. Comparison between experimental data and numerical model. a: full normalized curve, b: difference between numerical model and experimental normalized torque. [Color figure can be viewed in the online issue, which is available at wileyonlinelibrary.com.]

By means of the so called xyz method, independent variables may be established. From stoichiometry of the reaction, it can be argued that:

$$\begin{aligned}
 I &= I_0 - x \\
 R &= 2x - y \\
 P &= P_0 - y \\
 P^* &= y - 2z - q \\
 P_r^* &= z \\
 P_i^* &= q
 \end{aligned} \quad (4)$$

Obviously, from (4) it can be argued that independent variables are: $I(t)$, $R(t)$, $P_r^*(t)$, $P_i^*(t)$. Indeed:

$$\begin{aligned}
 x &= I - I_0 \\
 y &= 2(I - I_0) - R \\
 P &= P_0 + R - 2(I - I_0) \\
 P^* &= 2(I - I_0) - R - 2P_r^* - P_i^* \\
 z &= P_r^* \\
 q &= P_i^*
 \end{aligned} \quad (5)$$

The aim is to provide an analytical expression for vulcanized rubber, i.e., concentration of P^* with respect to time.

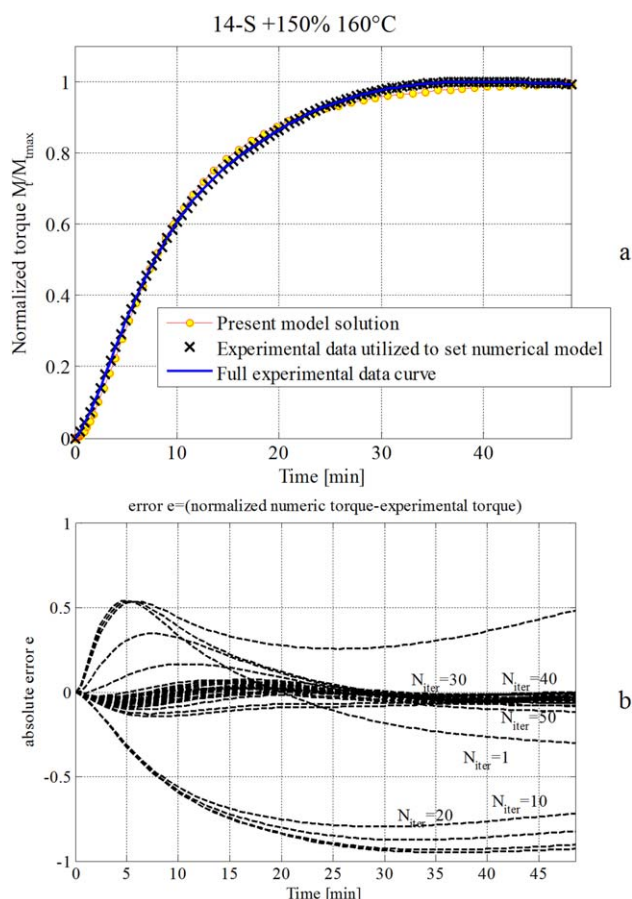


Figure 25. 14-S curing agent, 160°C. Comparison between experimental data and numerical model. a: full normalized curve, b: difference between numerical model and experimental normalized torque. [Color figure can be viewed in the online issue, which is available at wileyonlinelibrary.com.]

From (3) and (4), the following set of differential equations is deduced:

$$\begin{aligned}
 (a) \quad \frac{dI}{dt} &= -K_1 I \\
 (b) \quad \frac{dR}{dt} &= 2K_1 I - K_2 R P \\
 (c) \quad \frac{dP}{dt} &= -K_2 R P \\
 (d) \quad \frac{dP^*}{dt} &= K_2 R P - K_3 (P^*)^2 - K_4 P^* \\
 (e) \quad \frac{dP_r^*}{dt} &= K_3 (P^*)^2 \\
 (f) \quad \frac{dP_i^*}{dt} &= K_4 P^*
 \end{aligned} \quad (6)$$

(a), (b), and (c) form a system of differential equations in three variables which may be solved as follows. (a) may be solved immediately by separation of variables:

$$I = I_0 e^{-K_1(t-t_0)} \quad (7)$$

(b)–(c) combine in the following way:

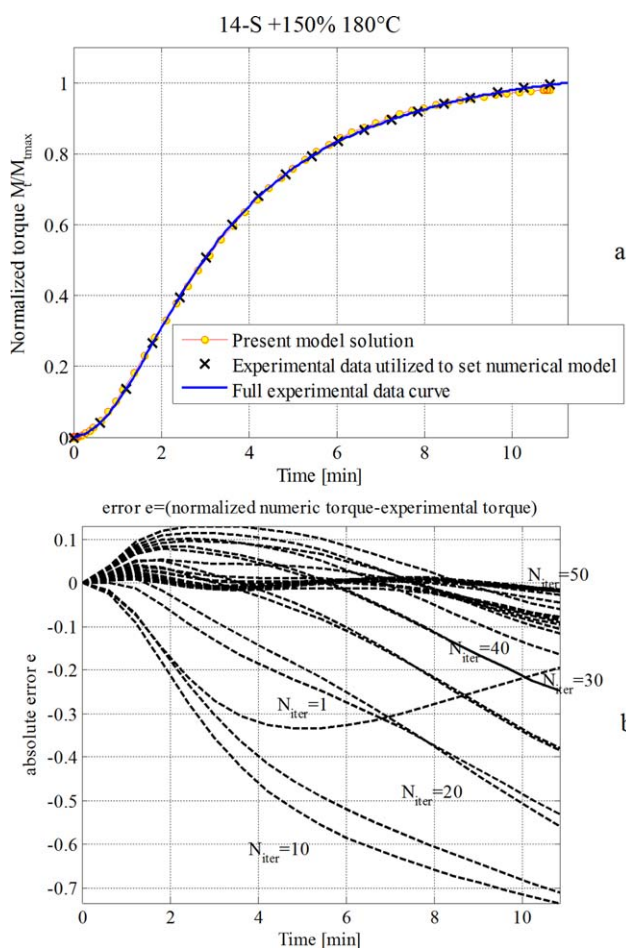


Figure 26. 14-S curing agent, 180°C. Comparison between experimental data and numerical model. a: full normalized curve, b: difference between numerical model and experimental normalized torque. [Color figure can be viewed in the online issue, which is available at wileyonlinelibrary.com.]

$$\frac{dR}{dt} - \frac{dP}{dt} = 2K_1 I = 2K_1 I_0 e^{-K_1(t-t_0)} \quad (8)$$

Differentiation of (c) results into:

$$\frac{d^2 P}{dt^2} = -K_2 R \frac{dP}{dt} - K_2 P \frac{dR}{dt} \quad (9)$$

From (8), remembering from (6) that $R = -\frac{1}{K_2 P} \frac{dP}{dt}$, the second order differential eq. (9) may be rewritten exclusively in terms of P as follows:

$$\frac{d^2 P}{dt^2} - \frac{1}{P} \left(\frac{dP}{dt} \right)^2 + K_2 P \frac{dP}{dt} + 2K_1 K_2 I_0 P e^{-K_1(t-t_0)} = 0 \quad (10)$$

The nonlinear differential eq. (10) may be solved numerically with a standard Runge–Kutta algorithm,³⁰ to find concentration $P(t)$. The knowledge of $P(t)$ allows the determination of quantity $R(t)$ and, from eq. (6)(d), P^* :

$$\frac{dP^*}{dt} = K_2 R(t) P(t) - K_3 (P^*)^2 - K_4 P^* \quad (11)$$

Equation (11) is again solved using a Runge–Kutta numerical approach.

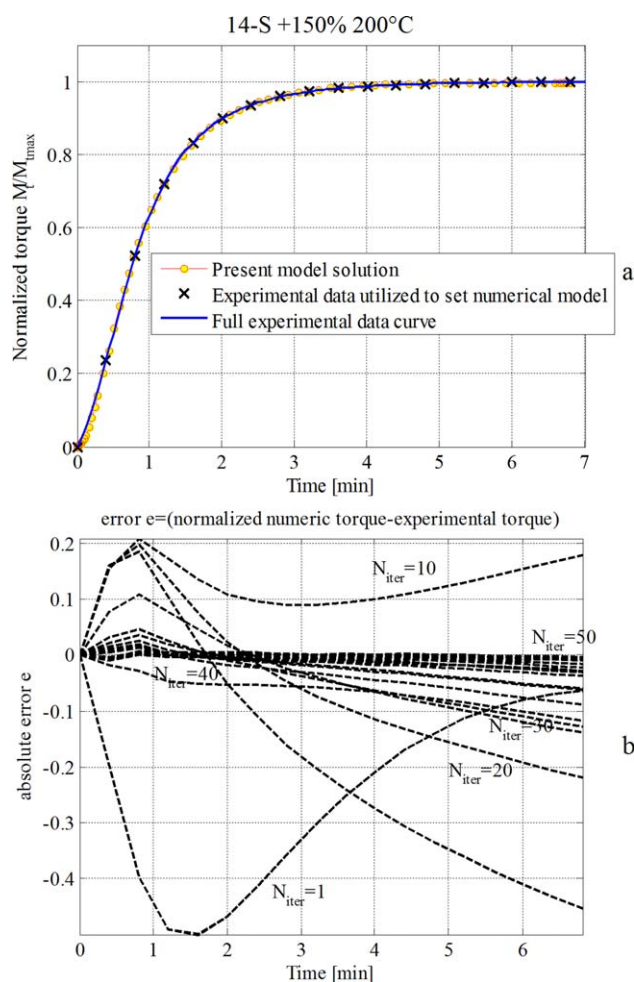


Figure 27. 14-S curing agent, 200°C. Comparison between experimental data and numerical model. a: full normalized curve, b: difference between numerical model and experimental normalized torque. [Color figure can be viewed in the online issue, which is available at wileyonlinelibrary.com.]

The combined application of eqs. (10) and (11) with least squares minimization, assuming as target curves to fit those obtained in the present experimental campaign, allows estimating kinetic constants entering into reaction scheme (3). When the capability of the model to fit reasonably well the experimental evidences is demonstrated, costing experimental campaigns could be avoided and, for different compounds, peroxides and mixtures of peroxides, numerical predictions may be used.

To perform a numerical optimization of the kinetic model proposed, experimental cure values are normalized dividing each point of the curve by the maximum torque values, so that experimental data are always within the range 0–1.

A comparison between present numerical curves and experimental data is provided from Figures 19(a)–27(a) for EPDM vulcanized with M3, BC-FF, and 14-S at 160, 180, and 200°C, respectively. The resultant kinetic constants found numerically are summarized in Table VI.

Table VI. Numerical Results Obtained After Least Square Optimization for Kinetic Constants K_i

	Temp	K_1	K_2	K_3	K_4
	[°C]	1/min	1/min	1/min	1/min
M3	160	0.055	0.190	0.00	0.00
	180	0.327	0.513	0.00	1.28 e-4
	200	2.284	1.319	1.13 e-4	8.70 e-4
BC-FF	160	0.069	0.301	0.00	0.00
	180	0.491	0.602	0.0001	0.0002
	200	2.401	2.330	0.0002	0.0001
14-S	160	0.048	0.191	0.00	0.00
	180	0.312	0.473	0.00	0.00
	200	2.221	1.126	9.46 e-5	3.45 e-5

As already pointed out, numerical curves are obtained using a nonlinear least square procedure, for which the convergence performance is evaluated from Figures 19(b)–27(b). In particular, in the figures, the absolute difference between normalized experimental torque and numerical predictions is represented, at successive iterations and at increasing instants between the initial and final time of experimentation. Obviously, as expected, passing from the initial iteration to the final, such difference decreases drastically, meaning that the least squares routine is achieving convergence. As it is possible to notice, the gap between numerical models and experimental data tends to zero for almost all the instants inspected, exception made for the initial simulation range, near scorch point. Here the experimental curve exhibits a sudden increase in the first derivative, meaning that the initiation of vulcanization is prone to occur. In any case, this stage is of little interest for the models proposed, which are designed for a reliable prediction of final reticulation level. In general, the agreement with experimental response seems rather promising, with an almost perfect superposition of the numerical curves with experimental data.

The convergence map of the least-square algorithm shows that after around 50 iterations the best fitting is always achieved, with errors in practice vanishing.

Considering the numerical values obtained for the first two constants K_1 and K_2 , reported in Table VI (the other constants are almost zero, indicating that no reversion is experienced) at two distinct temperatures, it appears interesting to plot the straight lines passing from such values in the Arrhenius plane. In such space, the horizontal axis is represented by the inverse of the absolute temperature, $1/T$, whereas the vertical axis is $\log(K_i)$, where K_i is the i^{th} kinetic constant. It is, indeed, commonly accepted that the variability of a single kinetic constant follows the so called Arrhenius law, which may be written as $K_i(T) = K_{i0} e^{\frac{E_{ai}}{R_g T}}$, where K_{i0} is the value of the i^{th} kinetic constant at an infinite temperature, E_{ai} is a constant typical of the reaction and R_g is the universal gas constant. In a $1/T$ - $\log(K_i)$ Cartesian plane, the Arrhenius law is thus represented by a straight line, intercepting vertical axis at $\log(K_{i0})$. Because experimental data are available at three distinct temperatures, and accepting that each single constant follows an Arrhenius law, it is possible

to sketch $K_i(T)$ lines in the $1/T$ - $\log(K_i)$ plane, for both peroxides under consideration and for the mixture of peroxides. Such representation is particularly useful from a practical point of view, because it allows a direct evaluation of the kinetic constants describing the velocity of the partial reactions at any vulcanization temperature. The straight lines numerically deduced are depicted in Figure 28. Subfigures refer to peroxides M3 (a), BC-FF (b), and 14-S (c), respectively. Numerical data of Table VI, utilized to plot the straight lines, are also indicated for the sake of clearness. To evaluate if the numerical approach proposed is in agreement with simplified procedures commonly used in practice, it is also possible to compare numerical results with commercial data available for both peroxides (note that no prediction may be done for the mixture) under consideration. In particular, Akzo Nobel furnishes in tabular form values of the kinetic constants of both BC-FF and 14-S at three different temperatures, corresponding to a half-time life equal to 0.1, 1, and 10 h, respectively. It is implicitly assumed that the reaction describing peroxide decomposition is of first order and that the single kinetic constant associated to such a reaction follows an Arrhenius law. It is very straightforward the deduction of the numerical values of the constants at the three temperatures considered, from the experimental knowledge of the half time life $t_{1/2}$, being simply $K_i \ln 2 = t_{1/2}$. No information is available for M3, which is indeed a mixture of peroxides.

Because in our numerical model, first and second reactions occur in series, and the first reaction produces $2R$ radicals, the comparison with the simplified practical approach above discussed, may be attempted considering the weighted average between constants K_1 and K_2 , i.e., plotting the straight line $1/3 \cdot (2 \log K_1 + \log K_2)$, again deduced from present numerical results and represented with a dash-dot line in Figure 28(b,c) for Perkadox BC-FF and Perkadox 14S-FL, respectively. In the same figures, data deduced from commercial catalogues provided by Akzo Nobel¹⁷ are represented with circles. As it is possible to notice, the agreement is almost perfect, meaning that the predictivity of the numerical procedure here presented is very promising. For the mixture of peroxides, a practical curve could be proposed in the same way, to be used directly by practitioners.

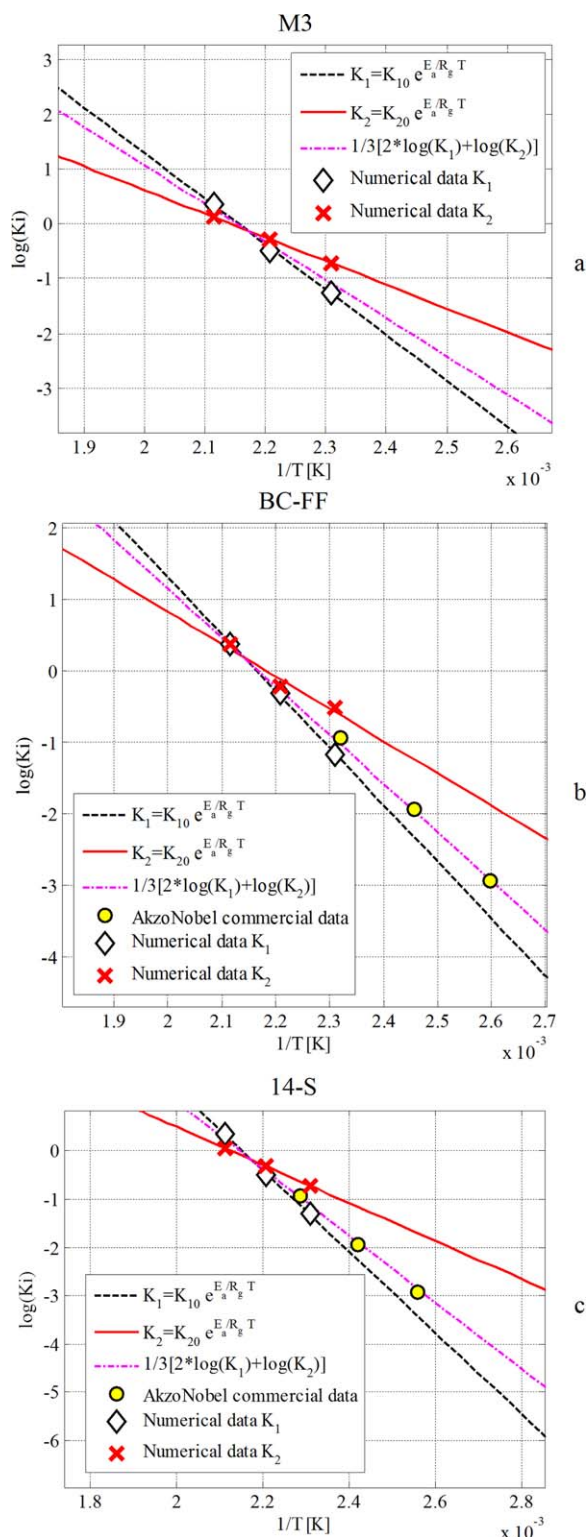


Figure 28. Linear regression interpolation of the kinetic constants K_1 and K_2 provided by the single differential equation model, the resultant linear regression obtained as weighted $K_1 + K_2$ and comparison with commercial data provided by Akzo Nobel for the peroxide under consideration. a: M3, b: BC-FF, c: 14-S. [Color figure can be viewed in the online issue, which is available at wileyonlinelibrary.com.]

CONCLUSIONS

An EPDM compound for medium voltage cables—commercially available in pellets or free-flowing and ready to be cured—was considered and several experimental tests (rheometer curves and mechanical characterizations) combined with a numerical assessment were performed with changing controlled curing temperatures, peroxide typologies, and peroxide concentration. Tests were replicated at temperature between 160 and 200°C, with data provided every 20°C, using two different peroxides and a mixture of three commercial peroxides at five different concentrations. A huge amount of experimental data (45 cure curves per 3 replicates) was obtained (one for each temperature, each peroxide and each concentration) and results were critically compared one each other, to have a quantitative indication for the most effective temperature and peroxide to be used during this kind of vulcanization.

From the extensive experimental campaign conducted by the authors, the following considerations may be drawn:

- Excluding results obtained at 160°C and with -50% concentrations, a linear correspondence between tensile strength of the vulcanized specimens and maximum torque is obtained independently from the curing agents utilized. This relationship may result extremely useful from a practical point of view, because it allows a prediction of the final properties of industrially produced items without a mechanical characterization performed at different temperatures. Such indirect evaluation could substitute, according to authors' opinion, direct *a posteriori* evaluations and could act as a benchmark for either compound producers or end users.
- As largely expected for rubber, the crosslinking rate increases by increasing the curing temperature. Conversely, literature results suggest that, generally, maximum torque and tensile strength should slightly decrease at high temperatures, a characteristic behavior that was not experienced by the authors in the present experimental campaign. However, from a qualitative analysis of experimental evidences, it can be argued that the optimal solution for the blend considered in the present tests is near 180°C.
- Perkadox BC-FF performs slightly better than M3 and Perkadox 14-S. Similar results are obtained with Perkadox 14-S only at 200°C, the latter being an obvious consequence of the slightly different half times exhibited by BC-FF and 14-S, being lower those relevant for BC-FF.
- An increase of peroxide concentration results into an increase of the crosslinking density, stabilizing at very high concentrations (in the range $+100\%$ – 150%). Values of tensile strength and maximum torque reach asymptotically a plateau within a range of concentration between 100 and 150%.
- The optimal concentration of the curing agent should be determined case by case, depending on the curing agent utilized. Nevertheless, it can be affirmed that, for the three cases analyzed in the present article, the optimal concentration should be searched between $+50\%$ and 100% considering also that an increase of curing agent results into an increase of productions costs.
- The typical decrease of tensile strength at large torque values documented in the literature²³ was not experienced in the

present set of experimental data. It is authors' opinion that this is a consequence of the utilization of peroxides concentrations unsuitable to put in evidence clearly such phenomenon. On the contrary, it can be stated that variations of the mechanical properties are not sensitive to increases or decreases of peroxides concentrations within a $\pm 20\%$ range per 100 g of polymer near the optimal concentrations.

In parallel, a numerical analysis was conducted by means of a non standard kinetic model, constituted by the most meaningful partial reactions occurring in series and parallel during peroxide curing.³⁰ A single nonlinear second order differential equation model was derived, where partial kinetic constants were evaluated by means of a Runge–Kutta approach in combination with non-linear least squares fitting. At the end of the vulcanization process, an estimation of the kinetic constants was obtained, which allowed a direct comparison with data usually adopted in common practice to evaluate the activity of the single peroxides at different temperatures. Finally it is interesting to notice that the utilization of the numerical model is crucial when dealing with the peroxides mixture, where simplified evaluations on the actual activity of the mixture are not known.

REFERENCES

1. Baldwin, F. P.; Ver Strate, G. *Rubber Chem. Technol.* **1972**, *45*, 709.
2. Pauling, L. *The Nature of the Chemical Bond*, 3rd ed.; Cornell University Press: Ithaca, NY, **1960**.
3. Di Giulio, E.; Ballini, G. *Kautsch. Gummi Kunstst.* **1962**, *15*, 6.
4. Keller, R. C. *Rubber Chem. Technol.* **1988**, *61*, 238.
5. Dluznieski, P. R. *Rubber Chem. Technol.* **2001**, *74*, 451.
6. Loan, L. D. *Rubber Chem. Technol.* **1967**, *40*, 149.
7. Seymour, D. C.; Krick, D. J. *Elastom. Plast.* **1979**, *11*, 97.
8. Vondoren, T. *Kautsch. Gummi Kunstst.* **1984**, *37*, 398.
9. Kosar, V.; Gomzi, Z. *Thermochim. Acta*, **2007**, *457*, 70.
10. Milani, G.; Milani, F. *Comput. Chem. Eng.* **2008**, *32*, 3198.
11. Milani, G.; Milani, F. *J. Appl. Polym. Sci.* **2009**, *111*, 482.
12. Milani, G.; Milani, F. *J. Appl. Polym. Sci.* **2010**, *115*, 1995.
13. Milani, G.; Milani, F. *Rubber Chem. Technol.* **2012**, *85*, 590.
14. Milani, G.; Milani, F. *Comput. Chem. Eng.* **2012**, *43*, 173.
15. Milani, G.; Milani, F. *Polym. Eng. Sci.* **2013**, *53*, 353.
16. Milani, G.; Milani, F. *J. Math. Chem.* **2010**, *47*, 229.
17. AkzoNobel. Brochure of organic peroxides, Available at: <http://www.akzonobel.com/polymer/>, **2012**.
18. Sun, X.; Isayev A. I. *Rubber Chem. Technol.* **2009**, *82*, 149.
19. ASTM D 2084-81—Annual Book of ASTM Standards 09.01, **1986**.
20. ASTM Standard D412. Standard test method for vulcanized rubbers and thermoplastic elastomers. Annual Book of Standards 09.01, **1986**.
21. Milani, G.; Milani, F. *J. Math. Chem.* **2011**, *48*, 530.
22. Milani, G.; Milani, F. *J. Appl. Polym. Sci.* **2012**, *124*, 311.
23. Coran, A. Y. In *Science and Technology of Rubber*; Eirich, R. F., Ed.; Academic Press: New York, **1978**; Chapter 7.
24. Hofmann, W. *Rubber Technology Handbook*; Hanser Publishers: Munich, **1989**.
25. Dees, M.; van Duin, M. *Rubber World*, August/September, **2008**.
26. van Duin, M. *Kautsch. Gummi Kunstst.* **2002**, *55*, 150.
27. Knox, B. E.; Palmer, B. *Chem. Rev.* **1961**, *61*, 247.
28. Dikland, H. G.; van Duin, M. In *Spectroscopy of Rubbers and Rubbery Materials*; Litvinov, V. M., De, P. P., Eds.; Rapra Technology Ltd: Shropshire, **2002**; p 207.
29. Hofmann, W. *Kautsch. Gummi Kunstst.* **1987**, *40*, 302.
30. Matlab User's Guide. Available at: <http://www.mathworks.com/products/matlab/>, **2007**.